Beating the "pros" with a semi-structural model of their own inflation forecasts*

Sergio Lago Alves
Bank of Canada

Waldyr Areosa
Banco Central do Brasil
and PUC-Rio

Carlos Carvalho
Kapitalo Investimentos
and PUC-Rio

January 5, 2026

Abstract

Professional inflation forecasts contain valuable information but exhibit information frictions. We extract improved forecasts by explicitly modeling these frictions using the US Survey of Professional Forecasters data, and find that forecast rigidity increases systematically with horizon, rising from near zero for backcasts to 0.81 beyond two quarters. In pseudo-real-time tests, our Resetting Nowcasts reduce mean squared errors by 50 percent relative to SPF averages. We derive a novel theoretical criterion showing that improved forecasts dominate when disagreement lies within an optimal interval determined by simple sufficient statistics, easily computable from any survey microdata. The criterion determines in advance the horizons where improved forecasts should dominate, without estimating friction parameters. This generalizes easily to other surveys and variables, providing a tractable method for identifying which forecast horizons offer the greatest potential for improvement.

JEL Codes: C53, E31, E37, C11

Keywords: inflation, survey expectations, information frictions, forecast disagreement

*For comments and suggestions we thank Olivier Coibion, Mike West, Oleksiy Kryvtsov, Roberto Billi, Tatjana Dahlhaus, Rodrigo Sekkel, Luis Uzeda, Kerem Tuzcuoglu, Elena Goldman and participants at the 2024 CEBRA Conference, 2023 NBER-NSF SBIES Conference, and seminars at Bank of Canada and Carleton University. The views expressed in this paper are those of the authors and do not necessarily reflect the views of Bank of Canada nor Banco Central do Brasil. E-mails: slagoalves@bank-banque-canada.ca, waldyr.dutra@bcb.gov.br, cvianac@econ.puc-rio.br.

1 Introduction

Monetary policy operates with long and uncertain lags, requiring policymakers to distinguish persistent from transitory inflation movements. Survey-based inflation expectations from professional forecasters provide valuable signals beyond headline inflation, as these analysts incorporate diverse data sources using models and judgment, and their collective forecasts are difficult to outperform in accuracy (e.g. Faust and Wright (2013)).[1] Yet extensive research documents that such forecasts exhibit information frictions rather than strict rationality (e.g. Coibion and Gorodnichenko (2015)).[2] This raises a fundamental question: can modeling these frictions extract the useful information embedded in professional forecasts and improve upon them?

We answer affirmatively firstly by performing an empirical exercise, based on estimating a model of forecast frictions, to extract useful information embedded in professionals' forecasts — what we call *Resetting Forecasts* —, showing that they strongly outperform US Survey of Professional Forecasters (SPF) consensus nowcasts, released by the Federal Reserve Bank of Philadelphia. Secondly, we provide a tractable theoretical framework to show that forecast disagreement is key in determining whether Resetting Forecasts dominate survey aggregates. Building on a model of noisy-dispersed information, we derive an optimal interval for disagreement: it must be sufficiently large to signal meaningful information dispersion, but not so large that forecasts become unreliable. The importance of this novel theoretical criterion is that it does not depend on estimating a model of forecast frictions. The optimal interval depends only on three sufficient statistics — unconditional variance of individual forecast errors, unconditional variance of average forecast errors, and unconditional variance of inflation —, which can be inferred from any survey dataset. This criterion correctly predicts the horizons where our empirical approach succeeds. And impotantly, this theoretical tool is generalizable to other surveys and forecasted varfiables, allowing for easier ex-ante identification of horizons with the greatest potential for improvement.

The empirical exercise uses a semi-structural state-space model that decomposes inflation into trend and cycle components using both the inflation time series and the term structure of SPF expectations.[3] The model incorporates information frictions that vary by forecast horizon—a feature

[1] Faust and Wright (2013) find that survey-based forecasts, such as Blue Chip and the SPF, outperform model-based forecasts, often by a wide margin. As Del Negro and Eusepi (2011) emphasize, professional forecasters have richer information sets that yield more precise readings of economic conditions. See also Ang et al. (2007), Croushore (2010), Faust and Wright (2009), Aiolfi et al. (2012), Rossi and Sekhposyan (2015), and Knotek II and Zaman (2017).

[2] See, among others, Mankiw and Reis (2002), Woodford (2003), Sims (2003), Mackowiak and Wiederholt (2009), Patton and Timmermann (2010), Patton and Timmermann (2011), Andrade and Le Bihan (2013), Coibion and Gorodnichenko (2012), Coibion and Gorodnichenko (2015), and Andrade et al. (2016).

[3] This follows the traditional literature on trend inflation and trend-cycle decompositions in the spirit of Beveridge

we show is essential for forecast accuracy. This approach yields three main contributions. First, we find that forecast rigidity increases systematically with horizon length, rising from essentially zero for backcasts to 0.81 beyond the two-quarters-ahead horizon. Models imposing uniform rigidity across horizons are strongly rejected by the data. This finding extends Coibion and Gorodnichenko (2015) by documenting substantial heterogeneity in information frictions across the term structure of expectations. Second, we establish that properly modeling these horizon-specific frictions enables significant improvements in forecast accuracy. In pseudo out-of-sample tests over 2006-2023, our quarterly Resetting Nowcasts dominate SPF averages, reducing mean squared errors by approximately 50 percent, with statistical significance under both Giacomini and White (2006) and Diebold and Mariano (1995) tests. At longer horizons, performance is comparable, consistent with theoretical predictions we develop. Third, our inflation decomposition also provides policy-relevant insights. We find that only a small portion of the 2021-2023 US inflation surge reflected permanent shifts in trend inflation. Most reflected medium-run transitory components, a finding with important implications for the appropriate monetary policy response.

Methodologically, we estimate a mixed-frequency state-space model combining monthly non-seasonally adjusted CPI data with quarterly SPF forecasts spanning backcasts through four-quarter-ahead projections. Using non-seasonally adjusted CPI data avoids complications from dealing with vintage revisions. And so, we explicitly model time-varying seasonality in the state-space model. The model nests a rational-forecaster benchmark and specifications with both uniform and horizon-varying rigidity parameters.

Our work relates to several strands of literature. Nason and Smith (2013) and Mertens and Nason (2018) also model forecast frictions and survey term structures but impose uniform rigidity and do not test forecast improvements. Jain (2018) examines SPF individual forecasts through the lens of loss aversion but finds no performance gains. Monti (2010) augments a DSGE model with judgmental forecasts to improve fit, whereas we use survey information to enhance estimation of the inflation process itself. More broadly, our approach connects to work extracting signals from cross-sectional forecast disagreement and to research on optimal forecast combination under model uncertainty.

In short, our paper makes three key contributions. First, we show that explicitly modeling information frictions in professional inflation forecasts allows one to extract the underlying signals and improve upon reported forecasts. Second, we demonstrate that forecast frictions are

and Nelson (1981), applied to inflation analyses by Stock and Watson (2007, 2010) and Schmitt-Grohe and Uribe (2022), among others.

horizon-specific and that accounting for this heterogeneity significantly enhances nowcasting and short-horizon forecasting accuracy. Third, we provide a simple theoretical criterion, based on readily available sufficient statistics, that identifies the horizons where improved forecasts are likely to dominate survey aggregates, offering a tractable and generalizable tool for analyzing survey expectations beyond the SPF.

The remainder of the paper proceeds as follows. Section 2 presents the model and characterizes SPF information sets.Section 3 describes data and estimation. Section 4 reports forecast performance tests. Section 5 develops the theory of forecast dominance. Section 6 concludes.

2 Modelling Strategy

In the US, SPF forecasts are quarterly released every second month of each quarter.[4]. For CPI, they aim at the quarterly CPI inflation, which is defined as the average-price inflation rate, i.e., the growth rate of the arithmetic mean of all three monthly CPI indexes in the quarter. If one wants to work with a linear state-space model, then one must obtain a log-linear approximation of this definition (see Section 2.2). As Mariano and Murasawa (2003) and Dahlhaus et al. (2017) show, the definition implies a (linearized) mapping from five lagged monthly rates into the average-index rates in a way that is impossible to account for when using pure quarterly data: the last two months from the previous quarter and all three months from the current quarter.

Therefore, on the one hand, the very nature of the average-price inflation rates requires dealing with a monthly frequency model for inflation. On the other hand, SPF forecasts are realized at a quarterly frequency. Therefore, a mixed-frequency framework seems more appropriate.

Whereas seasonally adjusted CPI inflation is subject to revisions, as new inflation information is released and seasonal patterns are updated, non-seasonally adjusted values are always final in the US. Therefore, to avoid the issues arising from dealing with the vintage available to forecasters in each period in the sample,[5] we opt to use non-seasonally adjusted CPI rates for inference, and include an internal filter based on Harrison and West (1997, chap. 8.2-8.4) and Harrison and Stevens (1975) to extract time-varying seasonal patterns.

[4] See Section 2.2 for more details.

[5] In the literature, this adjustment is always discretionary, varying from author to author, and generates questions on how old (or recent) the appropriate vintage must be in each quarter. For instance, Coibion and Gorodnichenko (2015) use real-time values available one year after the relevant time horizon. Faust and Wright (2013) use the real-time dataset of the Federal Reserve Bank of Philadelphia, recorded two quarters after the quarter to which the data refer. Lastly, Knotek II and Zaman (2017) treat the third monthly estimate of CPI prices as "truth," as registered in the St. Louis Fed's Archival Federal Reserve Economic Data (ALFRED).

In the remainder of this section, we describe our state-space model, used for inference. In the mixed-frequency context, we represent monthly periods with t, distinguishing them from quarterly periods q.

2.1 The Inflation Data-Generating Process

Following the literature on assessing frictions in professional forecasts, we consider a reduced-form structure for the inflation data-generating process (DGP).[6] Logarithmic monthly aggregate CPI inflation, non-seasonally adjusted, has four components that are unobserved to the econometrician: (i) a long-run (lr) persistent (unit root) trend component, π_t^{lr}; (ii) a medium-run (mr) transitory component, π_t^{mr}; (iii) a short-run (sr) transitory component π_t^{sr}; and (iv) a time-varying seasonal component, π_t^{sea}. Denoting aggregate inflation by π_t, we have:

$$\pi_t = \pi_t^{sea} + \pi_t^{sr} + \pi_t^{mr} + \pi_t^{lr}. \tag{1}$$

Indeed, as shown in Section 3.2, US CPI data strongly and significantly support the existence of two transitory components with different frequencies. In addition, Cogley and Sbordone (2008) and Faust and Wright (2013) highlight the importance of accounting for slow-moving changes in trend inflation (local means) for forecast purposes.[7]. In this sense, the two transitory components are allowed to have AR(1) dynamics, in which the inertial parameter of π_t^{sr} is smaller than that of π_t^{mr}, in absolute value. Long-run or trend inflation, π_t^{lr}, follows a random-walk, thus contributing to a loose-end level for inflation:

$$\begin{aligned} \pi_t^{sr} &= \rho_{sr}\pi_{t-1}^{sr} + \varepsilon_t^{sr} \quad ; \; \varepsilon_t^{sr} \sim N\left(0, \sigma_{sr}^2\right), \\ \pi_t^{mr} &= \rho_{mr}\pi_{t-1}^{mr} + \varepsilon_t^{mr} \quad ; \; \varepsilon_t^{mr} \sim N\left(0, \sigma_{mr}^2\right), \\ \pi_t^{lr} &= \pi_{t-1}^{lr} + \varepsilon_t^{lr} \quad ; \; \varepsilon_t^{lr} \sim N\left(0, \sigma_{lr}^2\right). \end{aligned} \tag{2}$$

where $|\rho_{sr}| < |\rho_{mr}| < 1$.

Defining the (logarithmic) seasonally adjusted monthly inflation rate, i.e. $\pi_t^{sa} \equiv \pi_t - \pi_t^{sea} = \pi_t^{mr} + \pi_t^{sr} + \pi_t^{lr}$ is also key when dealing with information coming from surveys. Note that our

[6] For instance, Coibion and Gorodnichenko (2015) consider a reduced-form AR(1) process for a macroeconomic variable in order to derive their noisy-information model for forecast rigidity. In light of the Lucas critique, we assume professional forecasters fully incorporate policy-implied dynamics into their best forecasts. Therefore, the flaws caused by Lucas (1976) critique will be greatly minimized when the estimated model is augmented with professional forecasts after modelling their frictions.

[7] In particular, Faust and Wright (2013) also consider a random walk formulation for trend inflation in one of their models.

approach is in line with Faust and Wright (2013) forecasting principles. In particular, they find that good forecasts must account for a slowly varying non-stationary trend inflation π_t^{lr} and model the inflation gap $\pi_t^{gap} \equiv \left(\pi_t^{sa} - \pi_t^{lr}\right)$ as a stationary component. In our specification, the inflation gap is accounted by $(\pi_t^{mr} + \pi_t^{sr})$, whose stationarity is ensured by the parameter restrictions $|\rho_{mr}| < 1$ and $|\rho_{sr}| < 1$.

Lastly, a time-varying seasonal component, π_t^{sea}, allows the model to capture changes in seasonal patterns due to reasons such as a smoothly evolving inflation seasonality pattern, or abrupt changes in the methodology for computing the consumption price index:

$$
\begin{aligned}
\pi_t^{sea} &= \pi_{1,t}^{sea}, \\
\pi_{1,t}^{sea} &= \pi_{2,t-1}^{sea} - \bar{\pi}_{t-1}^{sea} + \varepsilon_t^{sea} \qquad ; \ \varepsilon_t^{sea} \sim N\left(0, \sigma_{sea}^2\right) \\
\pi_{2,t}^{sea} &= \pi_{3,t-1}^{sea} - \bar{\pi}_{t-1}^{sea} - \tfrac{1}{T_y - 1}\varepsilon_t^{sea}, \\
&\vdots \\
\pi_{T_y,t}^{sea} &= \pi_{1,t-1}^{sea} - \bar{\pi}_{t-1}^{sea} - \tfrac{1}{T_y - 1}\varepsilon_t^{sea}, \\
\bar{\pi}_t^{sea} &\equiv \tfrac{1}{T_y}\textstyle\sum_{s=1}^{T_y} \pi_{s,t}^{sea}.
\end{aligned}
\tag{3}
$$

where T_y is the number of periods in a year ($T_y = 12$ for monthly frequency).

This approach to model a time-varying seasonal pattern closely follows the suggestions of Harrison and West (1997, chap. 8.2-8.4). By adding ε_t^{sea} to $\pi_{1,t}^{sea}$, subtracting $\frac{1}{T_y - 1}\varepsilon_t^{sea}$ from the remaining seasonal terms (see e.g. Harrison and Stevens (1975)) and subtracting the average seasonal component $\bar{\pi}_{t-1}^{sea}$ from all seasonal terms, we ensure the average $\bar{\pi}_t^{sea}$ is always zero.

All four DGP shocks ε_t^{sr}, ε_t^{mr}, ε_t^{lr} and ε_t^{sea} hit the economy at the beginning of month t. Even though the inflation DGP process may provide information to identify those shocks, the inference process also benefits from using extra information coming from professional forecasts. They can be particularly useful if available for multiple forecasting horizons, for revisions to the term structure of inflation forecasts provide valuable information about how forecasters perceive shocks to the inflation process. In response to shocks deemed transitory, survey participants revise their short-run forecasts, but leave those for longer horizons relatively unchanged. In contrast, shocks deemed persistent affect the whole term structure of inflation forecasts. Therefore, we assess the forecast formation process in the following section.

2.2 Forecasts and Information Sets

In the Survey of Professional Forecasters (SPF),[8] respondents provide quarterly forecasts for a set of economic quantities every other month of each quarter. Initially, since 1968, the survey was conducted by the American Statistical Association and the National Bureau of Economic Research. Beginning in the third quarter of 1990, the Federal Reserve Bank of Philadelphia took over the survey and adjusted its collecting dates to make sure respondents' information sets are updated with information concerning the previous quarter. SPF forecasts are collected and made public in the second month of each quarter (*pivot month*, henceforth), before the statistics for the first month of the quarter are released by the Bureau of Labor Statistics (BLS), which also compiles the Consumer Price Index (CPI), and U.S. Bureau of Economic Analysis (BEA). For monthly variables, therefore, the information set is updated up to the third month of the previous quarter. That is, respondents observe realised data with a 2-month delay.

Based on the Consumer Price Index (CPI) inflation compiled by the BLS, respondents provide forecasts on seasonally adjusted quarterly measures of the average-price rate for six horizons, i.e., the previous quarter (backcast), current quarter (nowcast) and future quarters up to four quarters ahead. In each quarter q, the quarterly average-price index P_q^{av} is defined as the arithmetic mean of all three monthly CPI indexes in the quarter, i.e. $P_q^{av} \equiv \frac{1}{3}\left(P_{1,q} + P_{2,q} + P_{3,q}\right)$. Therefore, the (gross) average-price rate is defined as $\Pi_q^{av} \equiv P_q^{av}/P_{q-1}^{av}$.[9]

To work with such SPF idiosyncrasies, we need to address two important points. The first one regards frequency conventions, as SPF forecasts are quarterly and CPI inflation rates are monthly. The second point deals with the information set available to respondents when they provide forecasts.

Considering the monthly frequency, let P_t^{sa} denote the true (not observed) seasonally adjusted CPI price index in each month. The monthly seasonally adjusted CPI (gross) inflation Π_t^{sa} is computed as $\Pi_t^{sa} = P_t^{sa}/P_{t-1}^{sa}$. If t is the pivot month, the seasonally adjusted (gross) quarterly average-price rate Π_t^{av} is computed as $\Pi_t^{av} = P_t^{av}/P_{t-3}^{av}$, where $P_t^{av} = \frac{1}{3}\left(P_{t+1}^{sa} + P_t^{sa} + P_{t-1}^{sa}\right)$. We aim to obtain a log-linearized mapping between Π_t^{av} and Π_t^{sa}. For that, lower case variables correspond to log-linearized versions of the original upper case variables, e.g. $\varkappa_t \equiv \log\left(\mathcal{X}_t\right)$.

As Mariano and Murasawa (2003) and Dahlhaus et al. (2017) show, log inflation $\pi_t^{av} \equiv \log\left(\Pi_t^{av}\right)$

[8] See more details in Croushore and Stark (2019).

[9] Respondents also provide annual end-of-year measures for the current year, as well as for up to two years ahead. However, since end-of-year forecasts need a different treatment to be incorporated in state-space models, we do not observe them in our inference exercises.

is approximated as follows:[10]

$$\pi_t^{av} \approx \frac{1}{3}\left[\pi_{t+1}^{sa} + 2\pi_t^{sa} + 3\pi_{t-1}^{sa} + 2\pi_{t-2}^{sa} + \pi_{t-3}^{sa}\right]$$

In Section 2.2.1, we elaborate on information sets.

2.2.1 Information Sets

Due to the delay in releasing monthly inflation rates π_t by the statistical agency, respondents only observe the history of inflation up to month $(t-2)$ when reporting to SPF.

As in Monti (2010), we reasonably assume respondents gather extra soft or hard public information between $(t-2)$ and right before π_{t-1} is released in period t, which allows for better conditional assessments of π_{t-1}^{sa} and π_t^{sa}. Let s_{t-1} and s_t summarize the extra public information gathered by specialists between periods $t-1$ and t.[11] These pieces of information allow forecasters an informed view of whether recent inflation developments are more transient or more persistent. Finally, we also assume s_t does not bring any extra information once π_t is released.

Now, we define two information sets. The first one is the full and updated information set $\mathcal{I}_t \equiv [\mathcal{I}_{t-1}, \pi_t] = [..., \pi_{t-3}, \pi_{t-2}, \pi_{t-1}, \pi_t]$, which is not available to SPF respondents. As Monti (2010) highlights, respondents actually have access to partial information sets $\mathcal{I}_t^* \equiv \left[\mathcal{I}_{t-1}^*, \pi_{t-2}, s_t\right] = [..., \pi_{t-3}, \pi_{t-2}, s_{t-1}, s_t]$, as they observe inflation realized up to month $(t-2)$ and collects intra-quarter soft or hard information, as mentioned before.[12] Therefore, partial information sets satisfy $\mathcal{I}_t^* = [\mathcal{I}_{t-2}, \mathcal{S}_t]$, where $\mathcal{S}_t = [s_{t-1}, s_t]$ represents the extra information gathered at periods $(t-1)$ and t.

Averaging across all individual forecasts, conditional on current partial information set $\mathcal{I}_t^*$ available to respondents, we define quarterly and monthly *Resetting Forecasts* as $E_t^*\pi_{t+h}^{av} \equiv E\left(\pi_{t+h}^{av}|\mathcal{I}_t^*\right)$ and $E_t^*\pi_{t+j}^{sa} \equiv E\left(\pi_{t+j}^{sa}|\mathcal{I}_t^*\right)$, where monthly horizons $j \in \{-1, 0, 1, 2, 3, ...\}$ are not necessarily coincident with SPF horizons $h \in \{-3, 0, 3, 6, 9, 12\}$. Likewise, conditional on the last full information set $\mathcal{I}_{t-2}$, we define quarterly and monthly expectations $E_{t-2}\pi_{t+h}^{av} \equiv E\left(\pi_{t+h}^{av}|\mathcal{I}_{t-2}\right)$ and $E_{t-2}\pi_{t+j}^{sa} \equiv E\left(\pi_{t+j}^{sa}|\mathcal{I}_{t-2}\right)$.

Because $\mathfrak{s}_{j,t}$ denote a non-observed variable capturing any information in $\mathcal{S}_t$, orthogonal to $\mathcal{I}_{t-2}$,

[10] See Online Appendix B for more details. The approximation also has the same intuition as in Crump et al. (2014), when they map quarterly growth rates into annual growth measures.

[11] This information may stem from the evolution of the general macroeconomic outlook, high-frequency information such as exchange rate movements and oil prices, announcements regarding future economic policies, and from news regarding price decisions of large firms.

[12] Paralleling Monti (2010), the information sets $\mathcal{I}_t^*$ are partial as they satisfy $\mathcal{I}_{t-2} \subset \mathcal{I}_t^* \subset \mathcal{I}_t$.

satisfying

$$E_t^* \pi_{t+j}^{sa} = E_{t-2} \pi_{t+j}^{sa} + \mathfrak{s}_{j,t} \tag{4}$$

Since $\mathcal{I}_t^* = [\mathcal{I}_{t-2}, \mathcal{S}_t]$, we obtain an important result, based on iterating expectations. It allows us to conclude that $E_t^* \pi_{t+j}^{sa}$ is centered around $E_{t-2} \pi_{t+j}^{sa}$ over time:

$$\begin{aligned} \int_{\mathcal{S}} E_t^* \pi_{t+j}^{sa} dP(\mathcal{S}_t) &\overset{definition}{=} \int_{\mathcal{S}} E\left(\pi_{t+j}^{sa} | \mathcal{I}_t^*\right) dP(\mathcal{S}_t) \overset{definition}{=} \int_{\mathcal{S}} E\left(\pi_{t+j}^{sa} | \mathcal{I}_{t-2}, \mathcal{S}_t\right) dP(\mathcal{S}_t) \\ &= \int_{\mathcal{S}} E\left(\pi_{t+j}^{sa} | \mathcal{I}_{t-2}, \mathcal{S}_t\right) P(\mathcal{S}_t) \, d\mathcal{S} = E\left(\pi_{t+j}^{sa} | \mathcal{I}_{t-2}\right) = E_{t-2} \pi_{t+j}^{sa} \end{aligned}$$

Since $\int_{\mathcal{S}} E_t^* \pi_{t+j}^{sa} dP(\mathcal{S}_t) = E_{t-2} \pi_{t+j}^{sa}$, equation (4) implies $\mathfrak{s}_{j,t}$ is unconditionally zero-meaned, i.e. $E(\mathfrak{s}_{j,t}) = 0$.[13] However, conditional on specific values for forecasts at $(t-1)$ and t, $\mathfrak{s}_{j,t}$ may have non zero conditional expectation.

Using the quarterly average-price rate approximation and $E_t^* \pi_{t+j}^{sa} = E_{t-2} \pi_{t+j}^{sa} + \mathfrak{s}_{j,t}$, resetting forecasts for $h \in \{-3, 0, 3, 6, 9, 12\}$ satisfy:

$$\begin{aligned} E_t^* \pi_{t+h}^{av} &= E_{t-2} \pi_{t+h}^{av} + \mathfrak{s}_{h,t}^{av} \\ E_t^* \pi_{t+h}^{av} &\equiv \tfrac{1}{3} E_t^* \left[\pi_{t+h+1}^{sa} + 2\pi_{t+h}^{sa} + 3\pi_{t+h-1}^{sa} + 2\pi_{t+h-2}^{sa} + \pi_{t+h-3}^{sa}\right] \\ \mathfrak{s}_{h,t}^{av} &\equiv \tfrac{1}{3} \left[\mathfrak{s}_{h+1,t} + 2\mathfrak{s}_{h,t} + 3\mathfrak{s}_{h-1,t} + 2\mathfrak{s}_{h-2,t} + \mathfrak{s}_{h-3,t}\right] \end{aligned} \tag{5}$$

2.2.2 Forecasters

There exists a unit mass of survey respondents $i \in (0, 1)$ that produce professional forecasts and know the structure and parameters describing the inflation DGP (1) – (3).[14] In the pivot month (second month) of each quarter, respondents form their quarterly forecast for the average price rate at the monthly horizon h, i.e. $\mathcal{F}_{i,t} \pi_{t+h}^{av}$ for $h \in \{-3, 0, 3, 6, 9, 12\}$. Reported forecasts are formed according to the process described below.

For any monthly horizon $j \in \{-1, 0, 1, 2, 3, ...\}$, respondents initially build private monthly expectations $E_{i,t}^* \pi_{t+j}^{sa}$. For each SPF horizon $h \in \{-3, 0, 3, 6, 9, 12\}$, they are aggregated into average quarterly expectations $E_{i,t}^* \pi_{t+h}^{av} \approx \frac{1}{3} E_{i,t}^* \left[\pi_{t+h+1}^{sa} + 2\pi_{t+h}^{sa} + 3\pi_{t+h-1}^{sa} + 2\pi_{t+h-2}^{sa} + \pi_{t+h-3}^{sa}\right]$.

Private expectations $E_{i,t}^* \pi_{t+j}^{sa}$ do not necessarily need to match the forecast $\mathcal{F}_{i,t} \pi_{t+h}^{av}$ respondents release to surveys. Before elaborating on this point, we assume that individual expectations are centered about Resetting Forecasts, defined as $E_t^* \pi_{t+h}^{av} \equiv \int_i E_{i,t}^* \pi_{t+h}^{av} di$.

[13] Note that $\mathfrak{s}_{j,t}$ behaves as if it were a disturbance that perturbs the strictly rational forecast, made with information up to $(t-2)$.

[14] Later on, we assume that the econometrician does not know the parameters, even though she understands the structure of the inflation DGP and the way respondents eventually fail to update their forecasts.

2.2.3 Forecast Rigidity

Coibion and Gorodnichenko (2015) show that forecast rigidity in the US is likely driven by information frictions (noisy/sticky) rather than competing formulations such as heterogeneous loss aversion to forecast errors (e.g. Capistran and Timmermann (2009a)). Therefore, the forecast rigidity we postulate is in the spirit of informational frictions models. The literature (e.g. Woodford (2003), Sims (2003), Mackowiak and Wiederholt (2009), Andrade and Le Bihan (2013), Coibion and Gorodnichenko (2015)) has shown the existence of an isomorphism, or quasi-isomorphism, between dynamic equations describing aggregate forecasts in models with sticky information (e.g. Mankiw and Reis (2002)), in which individual forecasters update their information set with a common probability, and in models with noisy information, in which individual forecasters obtain public and private signals to make their forecast. In this isomorphism, the Kalman gain γ in noisy information models plays the role of the probability $(1-\alpha)$ of updating the information set in sticky information models.

We do not set an instance on the ultimate source of information frictions, i.e. either noisy or sticky expectations, but depart from the literature by allowing for horizon-specific forecast rigidity. In Section 5.1, we provide theoretical grounds for horizon-specific Kalman gains in the context of a noisy-dispersed information model.

In this context, let $(1-\alpha_h)=\gamma_h$ denote either the probability of updating the information set (under sticky information) or the Kalman gain (under noisy information) when reporting forecasts for horizon $h \in \{-3,0,3,6,9,12\}$. Using the results shown in Section 2.2, the aggregate forecast for horizon $(t+h)$, $\mathcal{F}_t\pi^{av}_{t+h} \equiv \int_i \mathcal{F}_{i,t}\pi^{av}_{t+h}di$, evolves according to:

$$
\begin{aligned}
\mathcal{F}_t\pi^{av}_{t+h} &= (1-\alpha_h)\, E^*_t\pi^{av}_{t+h} + \alpha_h \mathcal{F}_{t-3}\pi^{av}_{t+h} \\
E^*_t\pi^{av}_{t+h} &= E_{t-2}\pi^{av}_{t+h} + \mathfrak{s}^{av}_{h,t} \\
\mathfrak{s}^{av}_{h,t} &= \tfrac{1}{3}\left[\mathfrak{s}_{h+1,t} + 2\mathfrak{s}_{h,t} + 3\mathfrak{s}_{h-1,t} + 2\mathfrak{s}_{h-2,t} + \mathfrak{s}_{h-3,t}\right]
\end{aligned}
\tag{6}
$$

where $E^*_t\pi^{av}_{t+h} = \int_i E^*_{i,t}\pi^{av}_{t+h}di$ is the latent Resetting Forecast for horizon $(t+h)$. Our assumptions can be thought of as a generalization of Monti (2010) approach. The author's model is a restricted version of (6), in which all rigidity parameters α_h are set to zero.

The recursive system that describes the formation of forecasts extends into the infinite horizon, as each forecast for horizon h depends on lagged forecast for horizon $(h+3)$, i.e. $\mathcal{F}_{t-3}\pi^{av}_{t+h} = L^3\mathcal{F}_t\pi^{av}_{t+h+3}$, where $L(\cdot)$ is the lag operator. Therefore, if one is to use (6) in econometric exercises

in which forecasts are observed up to monthly horizon H, the direct approach is truncating the recursion at a horizon $(H-3)$ and loose some available information. To cope with this issue, we show under weak assumptions that (6) at longer horizons is equivalent to an auto-contained equation system that does not depend on lagged forecasts of longer horizons.

Proposition 1 *If the degree of forecast rigidity for any horizon $h \geq H+3$ is constant, with $H \geq 0$, and there is no extra information disturbances for those longer horizons, i.e. $\alpha_h = \bar{\alpha}$ and $\mathfrak{s}_{h,t}^{av} = 0$ for $h \in \{H+3, H+6, ...\}$, then $\mathcal{F}_t \pi_{t+h}^{av}$ evolves according to an autoregressive system that does not depend on lagged forecasts for longer horizons:*

$$\begin{aligned} \mathcal{F}_t \pi_{t+h}^{av} &= \mathcal{F}_t \pi_{t+h}^{amr.} + \mathcal{F}_t \pi_{t+h}^{asr} + \mathcal{F}_t \pi_{t+h}^{alr} \\ \textit{where} & \end{aligned} \tag{7}$$

$$\begin{aligned} \mathcal{F}_t \pi_{t+h}^{amr.} &= (1-\bar{\alpha}) E_{t-2} \pi_{t+h}^{amr} + \bar{\alpha} (\rho_{mr})^3 \mathcal{F}_{t-3} \pi_{t-3+h}^{amr} \\ \mathcal{F}_t \pi_{t+h}^{asr.} &= (1-\bar{\alpha}) E_{t-2} \pi_{t+h}^{asr} + \bar{\alpha} (\rho_{sr})^3 \mathcal{F}_{t-3} \pi_{t-3+h}^{asr} \\ \mathcal{F}_t \pi_{t+h}^{alr} &= (1-\bar{\alpha}) E_{t-2} \pi_{t+h}^{alr} + \bar{\alpha} \mathcal{F}_{t-3} \pi_{t-3+h}^{alr} \end{aligned}$$

$$\begin{aligned} \pi_{t+h}^{amr} &\equiv \tfrac{1}{3} \left[\pi_{t+h+1}^{mr} + 2\pi_{t+h}^{mr} + 3\pi_{t+h-1}^{mr} + 2\pi_{t+h-2}^{mr} + \pi_{t+h-3}^{mr} \right] \\ \pi_{t+h}^{asr} &\equiv \tfrac{1}{3} \left[\pi_{t+h+1}^{sr} + 2\pi_{t+h}^{sr} + 3\pi_{t+h-1}^{sr} + 2\pi_{t+h-2}^{sr} + \pi_{t+h-3}^{sr} \right] \\ \pi_{t+h}^{alr} &\equiv \tfrac{1}{3} \left[\pi_{t+h+1}^{lr} + 2\pi_{t+h}^{lr} + 3\pi_{t+h-1}^{lr} + 2\pi_{t+h-2}^{lr} + \pi_{t+h-3}^{lr} \right] \end{aligned}$$

The proof is described in Online Appendix C.

Regarding this result, we highlight two points. First, as mentioned before, the latent variables on the left side of the second, third and fourth equations now depend on their own lagged values, i.e. $\mathcal{F}_{t-3} \pi_{t-3+h}^{amr} = L^3 \mathcal{F}_t \pi_{t+h}^{amr.}$, $\mathcal{F}_{t-3} \pi_{t-3+h}^{asr} = L^3 \mathcal{F}_t \pi_{t+h}^{asr.}$ and $\mathcal{F}_{t-3} \pi_{t-3+h}^{alr} = L^3 \mathcal{F}_t \pi_{t+h}^{alr}$, and not on lagged values of longer horizons. Second, the inertial parameters ρ_{mr} and ρ_{sr} of the DGP transitory components affect the dynamics of $\mathcal{F}_t \pi_{t+h}^{amr.}$ and $\mathcal{F}_t \pi_{t+h}^{asr}$.

2.3 Competing models

As detailed below, we consider seven competing model variations and test their in-sample and pseudo out-of-sample performances. In-sample comparisons, better detailed in Section 3, are done using the Log Marginal Likelihood (LML) statistics, using the full sample. Pseudo out-of-sample performance comparisons, better detailed in Section 4, are based on the models' forecast errors when compared to the SPF ones. For that, we use subsample windows to estimate the model, and forecast errors are computed using the subsample not used for estimation.

The first model we consider, which we call *Rational Forecasts (RFR)*, assumes there are no forecast rigidities, i.e. $\alpha_h = 0$ for monthly horizons $h \in \{-3, 0, 3, 6, 9, 12\}$. However, SPF forecasts have at least three different flavors, i.e., backcasts ($h = -3$), nowcasts ($h = 0$), and forecasts ($h \geq 3$). And so, it is reasonable to consider that forecasting rigidities might not be the same for all horizons.

Therefore, we also consider a broader class of six models with partially stable rigidity parameters, differing only in the horizon at which forecast rigidity parameters stabilize. That is, each *Sluggish Forecasts Horizon*$\mathcal{H}$ *(SF*$_{\mathcal{H}}$*)* model, for monthly horizon $\mathcal{H} \in \{-3, 0, 3, 6, 9, 12\}$, has specific rigidity parameters α_h for near monthly horizons $h < \mathcal{H}$ and constant parameters $\alpha_h = \bar{\alpha}_{\mathcal{H}}$ for $\forall h \geq \mathcal{H}$. Since model SF_{-3} is the one with constant rigidity, as it has $\alpha_h = \bar{\alpha}_{-3}$ for $\forall h \geq -3$, we call it the *Uniform Sluggishness (USL)* model. At the other extreme, model SF_{12} has specific rigidity parameters α_h for each forecasted horizon $h \in \{-3, 0, 3, 6, 9, 12\}$. We call it the *Full Sluggish Forecasts (FSF)* model, for it is the fully blown version of this class of forecast rigidity models.

3 Data Set and Inference

Inference exercises are carried out with a mixed frequency data set, i.e. monthly and quarterly series. We consider a sample from July 1990 to June 2023 to simultaneously estimate DGP and forecasting parameters. The sample begins in July 1990, as it was in the third quarter of 1990 that the Federal Reserve Bank of Philadelphia took over the Survey of Professional Forecasters (SPF), adjusting the survey respondents' information sets.

For the inflation metrics π_t, we only observe the monthly non-seasonally adjusted CPI inflation (US city average, All items), released by the US Bureau of Labor Statistics. For SPF quantities, we consider all six quarterly forecast means, i.e., for backcasts $\mathcal{F}_t \pi^{av}_{t-3}$, nowcasts $\mathcal{F}_t \pi^{av}_t$, and forecasts up to four quarters ahead $\mathcal{F}_t \pi^{av}_{t+h}$, for $h \in \{3, 6, 9, 12\}$. In monthly frequency, SPF forecasts time series are sparse, as we observe each realization every second month in the quarter, with two blanks between observations.[15]

Note that using SPF forecasts as additional information to estimate the DGP parameters is in line with Del Negro and Eusepi (2011), as they highlight that including professional forecasts among the observables is a way to exploit the forecasters' richer information set.

The model deals with logarithmized quantities, observing their appropriate time-aggregation.

[15] Here, we abstract from a potential Average Forecast bias originated by frequent entry and exit of individual forecasters, as highlighted in Capistran and Timmermann (2009b). Implicitly, we are assuming the potential bias will affect both the Average Forecasts as well as the Resetting Forecast, so that forecasting performance tests will not asymmetrically favor the latter nor the former.

For instance, a 1% monthly inflation rate is logarithmized into $100 \log(1.01) = 0.995$. On the other hand, since quarterly SPF forecasts are released in annualized units, we convert them into quarterly logarithmized units. That is, a 10% annualized quarterly SPF forecast is logarithmized into $100\frac{\log(1.10)}{4} = 2.38$.

3.1 Inference and Estimation

In each competing model, after accounting for restrictions on α_h, we simultaneously estimate parameters for the forecasts' laws of motion $\Theta_f \equiv [\alpha_{-3}, \alpha_0, \alpha_3, \alpha_6, \alpha_9, \alpha_{12}, \sigma_{\mathfrak{s}}]$ and DGP process $\Theta_d \equiv [\rho_{mr}, \rho_{sr}, \sigma_{mr}, \sigma_{sr}, \sigma_{lr}, \sigma_{sea}]$.

For inference, we use the equations describing the inflation DGP $(1-3)$ and those describing the forecast rigidity processes (6) for all SPF horizons $h \in \{-3, 0, 3, 6, 9, 12\}$, and conveniently model the latent variable $\mathfrak{s}_{h,t}$ as a white noise disturbance $\mathfrak{s}_{h,t} \sim N\left(0, \sigma_h^2\right)$. Lastly, for inference pragmatism, we need minor assumptions to simplify estimation in this mixed-frequency estimation environment, as SPF information is more sparse than monthly information. In Online Appendix D, we describe those assumptions and show how they affect the estimated forecast system.

As SPF forecasts are only observed in the second month of each quarter, we treat them as having missing observations in the first and third months of each quarter. Therefore, estimation is carried out with a mixed-frequency Bayesian approach, using the Kalman filter to deal with missing observations.[16] For the Kalman filter initialization, we use a diffuse filter. We employ a Metropolis-Hastings MCMC sampler, with 2 independent chains of 1 million draws, disregarding the first 50% as burn-in. The joint prior is given by the product of uniform densities, with sufficiently wide supports. In this case, support upper bounds must be large enough so that the posterior density mimics the likelihood function. On the other hand, extremely large supports generate inefficiencies during MCMC draws. Therefore, we have to balance efficiency versus avoiding truncating the likelihood function. For inertia (ρ_{mr}, ρ_{sr}) and rigidity (α_h) parameters, we consider their natural supports bounded between 0 and 1. As for the remaining standard deviation parameters, we considered sufficiently large supports in the non-negative space, so that posterior densities are not truncated.

To closely mimic the information set restrictions faced by econometricians who want to improve over realized SPF forecasts in real-time, we adjust the information set for the Kalman filter to obtain more realistic likelihood evaluations. In each month t in the sample, the information set

[16] See e.g. Prado and West (2010, Section 4.3.3) and Durbin and Koopman (2012, Section 4.10) for a discussion on Kalman filtering with missing observations.

is updated up to current SPF forecasts $\mathcal{F}_t \pi^{av}_{t+h}$ (as well as backcasts and nowcasts) and 2-month lagged inflation realizations π_{t-2}.

Using the Kalman filter for likelihood evaluation, we consider information sets comprising all contemporaneous SPF forecasts $\mathcal{F}_t \pi^{av}_{t+h}$ and 2-month lagged (non-seasonally adjusted) headline inflation π_{t-2}. In a T-sized sample, the filter observes $6T/3$ quarterly SPF forecasts and T monthly inflation observations, from π_{-1} to π_{T-2}.

3.2 Estimates

Table 1 shows the estimated parameters for the forecasts' laws of motion and DGP, including their modes and 90% credible intervals, for all competing models: *Rational Forecasts (RFR)*, and *Sluggish Forecasts Horizon* $\mathcal{H}$ *(SF*$_{\mathcal{H}}$*)* models, for monthly horizon $\mathcal{H} \in \{-3, 0, 3, 6, 9, 12\}$.

Notice that models that impose zero forecast rigidity for all horizons (RFR) or near constant forecast rigidity (SF_{-3} and SF_0) perform much poorer than those that allow at least backcasts, nowcasts and forecasts to have specific parameter rigidities. Indeed, the model SF_{-3} is the simplest one that splits rigidity parameters into backcasts, nowcasts, and forecasts, and has a much larger LML than those of models RFR, SF_{-3}, and SF_0.

The left panel of Figure 1 depicts LML statistics for each competing model. The highest LML model (SF_6) is highlighted with a red bar. The right panel of Figure 1 compares forecast rigidity parameters for Restricted (with $\alpha_{-3} = 0$) models SF_6 (black line), SF_9 (red dotted and crosses) and SF_{12} (blue dashed with circles). The panel shows rigidity parameters at the posterior mode, in addition to SF_6 90% credible intervals. Note that the degree of forecast rigidity is very close to zero for backcasts, concavely increases for longer horizons, and seems to stabilize at distant horizons.

Since the SF_6 model has the largest LML statistics, we show its parameters marginal posterior density plots (black lines) in Figure 2. All parameters seem to be perfectly identified, especially when considering that we use flat priors (red dashed lines).

Table 1: MCMC Estimates - Testing Forecast Rigidity Stability

	RFR	SF_{-3}	SF_0	SF_3	SF_6	SF_9	SF_{12}
LML	6314.5	6324.5	6376.3	6439.0	6471.0	6467.3	6467.8
α_{-3}	0	0.220 (0.18,0.26)	0.000 (0.00,0.03)	0.032 (0.00,0.08)	0.060 (0.00,0.11)	0.058 (0.00,0.11)	0.064 (0.00,0.11)
α_0	0	0.220 (0.18,0.26)	0.332 (0.30,0.37)	0.416 (0.37,0.46)	0.393 (0.34,0.45)	0.393 (0.33,0.45)	0.395 (0.33,0.45)
α_3	0	0.220 (0.18,0.26)	0.332 (0.30,0.37)	0.752 (0.72,0.78)	0.743 (0.71,0.77)	0.745 (0.71,0.77)	0.748 (0.71,0.78)
α_6	0	0.220 (0.18,0.26)	0.332 (0.30,0.37)	0.752 (0.72,0.78)	0.825 (0.80,0.85)	0.829 (0.80,0.85)	0.828 (0.80,0.85)
α_9	0	0.220 (0.18,0.26)	0.332 (0.30,0.37)	0.752 (0.72,0.78)	0.825 (0.80,0.85)	0.817 (0.79,0.84)	0.812 (0.78,0.83)
α_{12}	0	0.220 (0.18,0.26)	0.332 (0.30,0.37)	0.752 (0.72,0.78)	0.825 (0.80,0.85)	0.817 (0.79,0.84)	0.842 (0.81,0.86)
$\sigma_{\mathfrak{s}}$	0.020 (0.02,0.02)	0.018 (0.02,0.02)	0.028 (0.02,0.03)	0.067 (0.06,0.08)	0.078 (0.07,0.09)	0.077 (0.07,0.09)	0.078 (0.07,0.09)
ρ_{mr}	0.580 (0.55,0.60)	0.814 (0.75,0.86)	0.578 (0.56,0.60)	0.882 (0.85,0.90)	0.927 (0.91,0.94)	0.924 (0.91,0.94)	0.930 (0.91,0.94)
ρ_{sr}	−0.302 (−0.36,−0.24)	0.337 (0.25,0.40)	−0.324 (−0.41,−0.25)	0.107 (0.02,0.19)	0.134 (0.06,0.21)	0.130 (0.05,0.20)	0.135 (0.05,0.21)
σ_{mr}	0.134 (0.12,0.15)	0.052 (0.04,0.08)	0.185 (0.17,0.21)	0.095 (0.08,0.11)	0.078 (0.06,0.09)	0.079 (0.07,0.10)	0.078 (0.06,0.09)
σ_{sr}	0.246 (0.23,0.27)	0.224 (0.21,0.24)	0.208 (0.19,0.23)	0.221 (0.20,0.24)	0.225 (0.21,0.24)	0.225 (0.21,0.24)	0.225 (0.21,0.24)
σ_{lr}	0.007 (0.01,0.01)	0.006 (0.00,0.01)	0.009 (0.01,0.01)	0.005 (0.00,0.01)	0.005 (0.00,0.01)	0.005 (0.00,0.01)	0.005 (0.00,0.01)
σ_{sea}	0.063 (0.05,0.07)	0.209 (0.19,0.23)	0.051 (0.04,0.06)	0.044 (0.03,0.06)	0.040 (0.03,0.05)	0.040 (0.03,0.05)	0.040 (0.03,0.05)

Notes: The statistics are modes, 90% credible intervals and Log Marginal Likelihood (LML). Mixed frequency sample: July 1990 to June 2023. Net sample size: 1188 observations. In-sample rate of missing observations: 57.1%. Observed variables: monthly headline CPI (non-seasonally adjusted) rate, quarterly SPF backcast, nowcast, and forecasts up to 4 quarters ahead for quarterly CPI rates. Metropolis-Hastings MCMC with 2 independent chains of 1000000 draws and 50% burnin rate. Rational Forecasts (RFR) model imposes fixed $\alpha_h = 0$ *for all horizons* $h \geq -3$. *Sluggish Forecasts Horizon* $\mathcal{H}(SF_{\mathcal{H}})$ *models, for monthly horizon* $\mathcal{H} \in \{-3, 0, 3, 6, 9, 12\}$, *have specific and different rigidity parameters* α_h *for monthly horizons* $h < \mathcal{H}$ *and fixed parameters* $\alpha_h = \bar{\alpha}_{\mathcal{H}}$ *for all horizons* $h \geq \mathcal{H}$. *Underlined modes refer to fixed parameters at* $h > \mathcal{H}$.

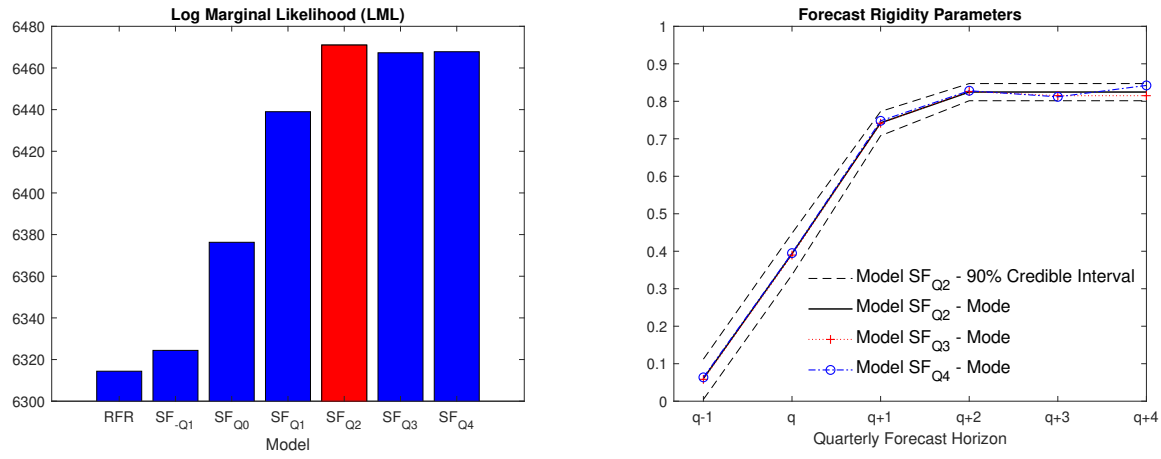


Figure 1: Testing Rigidity Stability in Forecast Horizons

Notes: LML stands for Log Marginal Likelihood. The highest LML model (SF_6) is highlighted with a red bar. Sluggish Forecasts Horizon $\mathcal{H}$ ($SF_{\mathcal{H}}$) models, for monthly horizon $\mathcal{H} \in \{-3, 0, 3, 6, 9, 12\}$, have horizon-specific rigidity parameters α_h for horizons $h < \mathcal{H}$ and fixed parameters $\alpha_h = \bar{\alpha}$ for all horizons $h \geq \mathcal{H}$.

Using the SF_6 model's posterior distribution, Figure 3 shows its underlying DGP components from July 1990 to June 2023. Solid lines show inference based on the mode parameters, while dotted lines show 90% credible intervals based on the parameters' asymmetric distribution.

The left panel on the top row compares the model-based long-run trend inflation to the Adjusted SPF 10-Year CPI inflation rate. Since the SPF 10-Year CPI inflation rate is meant to be the forecast for the average annual rate from the current year until 10 years in the future, we compute the adjusted forecast by discounting the available forecasts for the immediately shorter horizon nearest to the 10-Year ahead horizon. That is, we discount the SPF 2-Year Forecast until 2005:Q1, and from 2005:Q2 on, we use the SPF 5-Year forecast for discounting, adjusting the forecasts' time spans. We highlight that the Adjusted SPF 10-Year CPI inflation rate is not used as an observed variable in inference exercises, and is only shown here for comparison purposes.

A first thing to highlight is how stable and well-behaved the model-based long-run trend inflation has evolved, whereas the SPF 10-Year CPI inflation rate presents more erratic fluctuations. Since 2000, the model-based long rate has been stable under a 2.20-2.50 percent range. As for the stationary medium-run component, with a half-life of about $\frac{\log(0.5)}{\log(0.92)} \approx 8.3$ months, the results suggest this is the one increasing since September 2020, during the inflation surge caused by the COVID-19 pandemic, while the long-rate has remained stable at a 2.30 percent level. The stationary short-run component, with a half-life of about $\frac{\log(0.5)}{\log(0.12)} \approx 0.3$ months, became slightly more volatile since the pandemic struck, but not as strongly as it was during the world financial crisis.

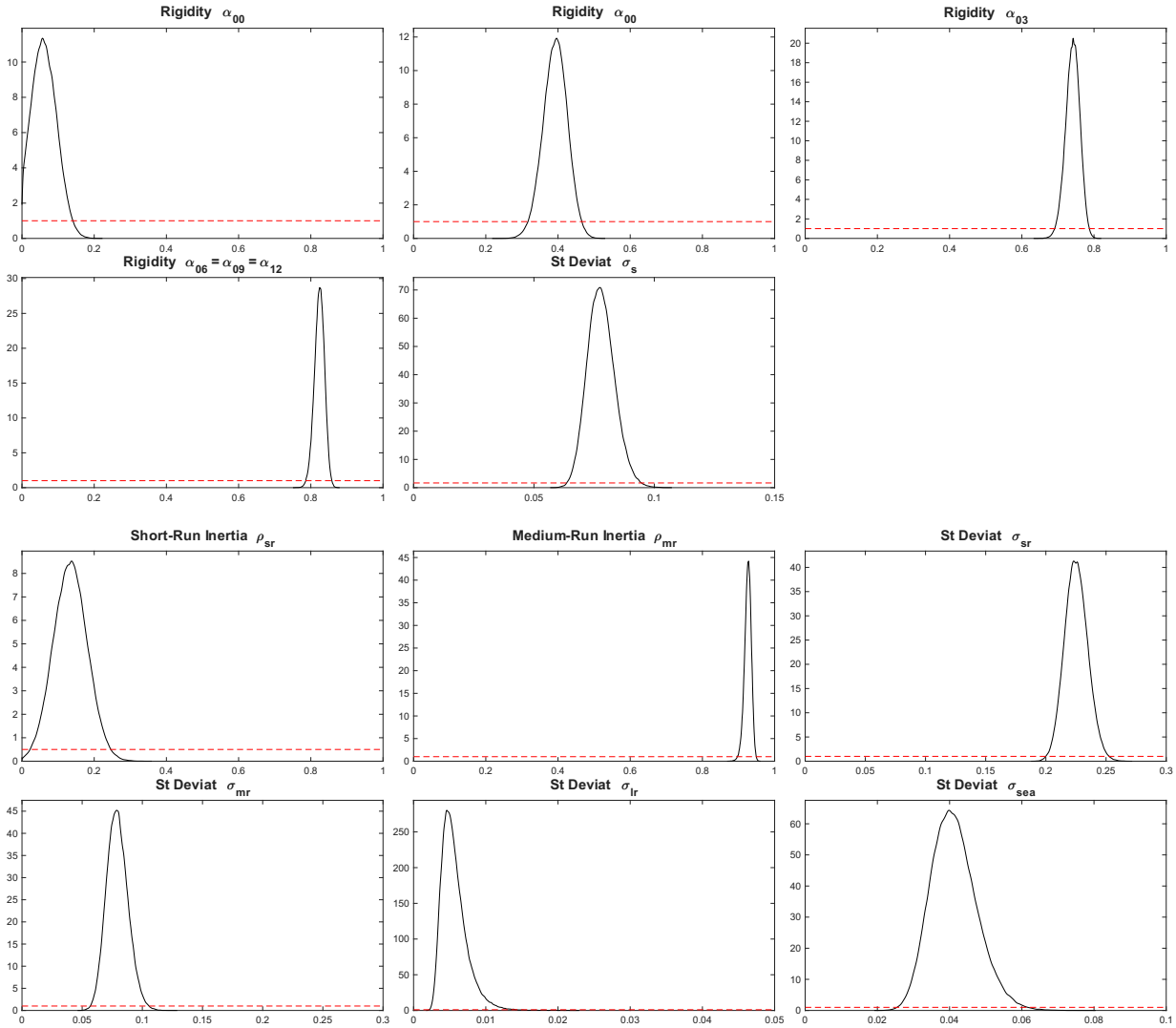


Figure 2: Density Plot - Restricted SF_6 Model

Notes: SF_6 model. Marginal posterior density (black lines), Marginal prior density (red dashed lines). Metropolis-Hastings MCMC with 2 independent chains of 1000000 draws and 50% burnin rate. Mixed frequency sample: July 1990 to June 2023. Net sample size: 1188 observations. In-sample rate of missing observations: 57.1%. Observed variables: monthly headline CPI (non-seasonally adjusted) inflation rate, Quarterly SPF backcast, nowcast, and forecasts up to 4 quarters ahead for quarterly CPI inflation rates.

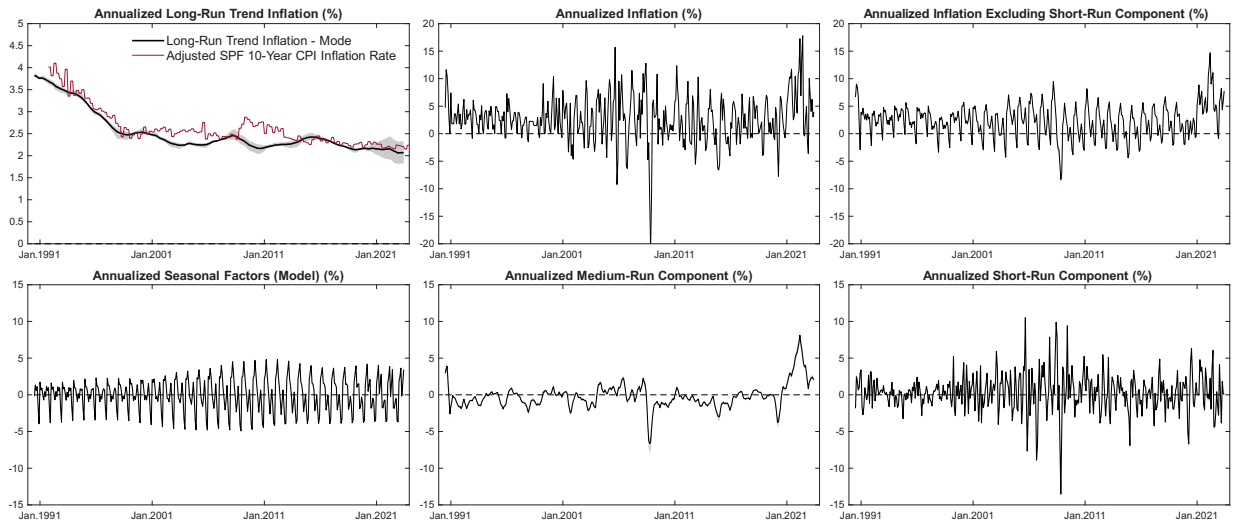


Figure 3: DGP Components - Restricted SF6 Model

Notes: SF_6 model's DGP components obtained from Kalman filter smoothed distribution, aggregated into annualized monthly frequency, from July 1990 to June 2023. Solid lines show inference based on mode parameters. Dotted lines show 90% credible intervals based on the parameters' asymmetric distribution. The Adjusted SPF 10-Year CPI inflation rate was computed by discounting the SPF 2-Year Forecast (until 2005:Q1). From 2005:Q2 on, we use the SPF 5-Year forecast for discounting. The Adjusted SPF 10-Year CPI inflation rate is not used as an observed variable in inference exercises, and is only shown here for comparison purposes.

Also, notice the Kalman filter interprets a sizeable share of inflation fluctuations as short-run components. In fact, as shown in the right panel on the top row, it is much easier to visually identify trends, transitory components, and the seasonal pattern after excluding the short-run component. This task is not that easy for the full non-seasonally adjusted inflation rate, depicted in the middle panel on the top row. As for the time-varying seasonal pattern, the model does a good job of endogenously capturing its evolution. This result is important, as we do not observe seasonally adjusted CPI inflation in inference exercises.

In Schmitt-Grohe and Uribe (2022), the authors do not decompose transitory inflation components into short and medium run, and do not use forecast data. They find that the only way to obtain a stable long-run component post COVID-19 and attribute the major fraction of observed post-COVID-19 inflation to transitory components is to expand the sample to include the first half of the 20th century. Using postwar data, their model interprets the recent inflation surge as mostly coming from long-run components. In our model, we do not need to use such a large sample to obtain the same conclusion. With our approach, on the other hand, we only use data starting from July 1990 and still manage to find a stable long-run component and attribute the recent inflation surge to transitory components.

4 Forecast Performance

As one of our main goals is to obtain relevant information to improve forecast accuracy, we now proceed to a simple comparison between SPF Average Forecasts $\mathcal{F}_t\pi^{av}_{t+h}$, for all horizons $h \in \{-3, 0, 3, 6, 9, 12\}$, against model-based pseudo out-of-sample Resetting Forecasts $E^*_t\pi^{av}_{t+h}$. In Section 5, we present a proposition on forecasting performance, showing the necessary theoretical conditions for Resetting Forecasts to dominate Average Forecasts.

We start from model forecasts of logarithmized monthly rates $E^*_t\pi^{sa}_{t+j} = E_{t-2}\pi^{sa}_{t+j} + \mathfrak{s}_{j,t}$, and build the annualized rates in levels. As explained in Section 2.2, the extra terms $\mathfrak{s}_{j,t}$ are not simple econometrics error terms, for they convey intra-quarter soft and higher frequency information, i.e. information in $\mathcal{S}_t$, orthogonal to $\mathcal{I}_{t-2}$. As we find in this section, $\mathfrak{s}_{j,t}$ is a key forecast component for nowcasts. Even though we find $E_{t-2}\pi^{sa}_{t+j}$, nowcasting performance is somehow better than that of pure SPF nowcasts, $E^*_t\pi^{sa}_{t+j}$ is strongly and significantly better than SPF nowcasts. As the results suggest, $\mathfrak{s}_{j,t}$ adds important nowcasting value into $E^*_t\pi^{sa}_{t+j}$.

Note that the logarithmized forecasts' laws of motion (6), i.e. $\mathcal{F}_t\pi^{av}_{t+h} = (1-\alpha_h)\, E^*_t\pi^{av}_{t+h} + \alpha_h\mathcal{F}_{t-3}\pi^{av}_{t+h}$, imply that SPF forecasts $\mathcal{F}_t\pi^{av}_{t+h}$ and model-based forecasts $E^*_t\pi^{av}_{t+h}$ are nested. That is, they are the same when $\alpha_h = 0$.[17] Therefore, the conditional approach of the Giacomini and White (2006) (GW) test is the most appropriate in our case. Even though the usual Diebold and Mariano (1995) (DM) test is not suited for nested models comparisons, we also show its results for robustness checks.

We run pseudo out-of-sample forecasts performance comparisons in two exercises, differing in the type of estimation window. The first one consists of estimating the models with rolling window samples of increasing size, with at least 15 years of monthly mixed-frequency data. That is, we set the beginning of each sample at the same period, and observe monthly (non-seasonally adjusted) headline CPI inflation rates and SPF quarterly forecasts for the 6 forecasting horizons $h \in \{-3, 0, 3, 6, 9, 12\}$. However, the Giacomini and White (2006) test is originally based on forecasts built after estimating models with fixed-size rolling window samples. Therefore, our second exercise uses samples with 15 years of monthly data. In this case, each fixed estimation window has always 180 observations of monthly (non-seasonally adjusted) headline CPI inflation

[17] Indeed, after solving for the expectations components with any assumption regarding rationality or bounded rationality, the solution for expectation terms always have the form $E^*_t\pi^{av}_{t+h} = A_h\mathcal{X}_{t-1} + B_h\xi_t$, where $\mathcal{X}_{t-1}$ is a vector of lagged state variables in state-space form, ξ_t is a vector os contemporaneous shocks, and A_h and B_h are row vectors based on the model parameters. Since $\mathcal{F}_{t-3}\pi^{av}_{t+h}$ already is a lagged state variable, for it is the 3-month lagged value of $\mathcal{F}_t\pi^{av}_{t+h+3}$, the solution for $\mathcal{F}_t\pi^{av}_{t+h}$ must have the form $\mathcal{F}_t\pi^{av}_{t+h} = (1-\alpha_h)\,(A_h\mathcal{X}_{t-1} + B_h\xi_t) + \alpha_h\mathcal{F}_{t-3}\pi^{av}_{t+h} = (1-\alpha_h)\,A_h\mathcal{X}_{t-1} + \alpha_h\mathcal{F}_{t-3}\pi^{av}_{t+h} + (1-\alpha_h)\,B_h\xi_t$. Hence, the linear regression equations for $\mathcal{F}_t\pi^{av}_{t+h}$ and $E^*_t\pi^{av}_{t+h}$ as functions of lagged state variables are nested.

rate,[18] as well as 6×60 observations of quarterly SPF forecasts. Therefore, each fixed window always has a total of $180 + 6 \cdot 60 = 540$ observations. Each increasing-size sample, on the other hand, has at least 540 observations.

In both exercises, we set the samples to start in Januaries and end in Decembers, mimicking an econometrician who reestimates her model once a year, after BLS releases the previous December's inflation rate. And so, we use the same estimated parameters throughout each year, before reestimating them in the next January. Since the Philadelphia Fed only took over the SPF in the third quarter of 1990, increasing size samples all begin in January 1991. The first increasing-size sample spans from January 1991 to December 2005, and the last one spans from January 1991 to December 2021. As for the 15-year window samples, the first one spans from January 1991 to December 2005, and the last one spans from January 2007 to December 2021. Both exercises set their testing windows at January 2006 to June 2023.

The estimation windows, as well as the testing window, were subjected to methodological and stressful events that might have had important temporary and permanent effects on US inflation dynamics and volatility, due to demand, supply, and policy changes.[19] Despite those methodological and stressful events, we do not exclude any period from the analyses and keep all forecasting errors in the analyses.

In each exercise, we estimate 13 parameters, i.e. 7 for the forecasts' laws of motion $\Theta_f \equiv [\alpha_{-3}, \alpha_0, \alpha_3, \alpha_6, \alpha_9, \alpha_{12}, \sigma_{\mathfrak{s}}]$ and 6 for the DGP $\Theta_d \equiv [\rho_{mr}, \rho_{sr}, \sigma_{mr}, \sigma_{sr}, \sigma_{lr}, \sigma_{sea}]$. As previously detailed, models $\text{SF}_{\mathcal{H}}$ impose $\alpha_h = \bar{\alpha}_{\mathcal{H}}$, for all horizons $h \geq H$.

For each model, in both exercises, we start by computing pseudo out-of-sample forecasts for logarithmized quantities using the models' filtered distributions to retrieve (seasonally adjusted) $E_t^* \pi_{t+h}^{av}$ and $E_{t-2} \pi_{t+h}^{av}$, for $h \in \{-3, 0, 3, 6, 9, 12\}$. We design the information set so that filtered distributions provide what econometricians would obtain as seasonally-adjusted forecasts in each period after observing recent available information. That is, at each month $t \in [1, ..., T]$, the available information set contains past realizations of monthly headline (non-seasonally adjusted)

[18] Recall that, in estimating the models, we only observe SPF forecasts and headline (non-seasonally adjusted) CPI inflation, and so seasonal adjustments are internally carried out in the model. As mentioned before, this strategy avoids the issue of dealing with vintages of seasonally adjusted CPI inflation in estimation exercises.

[19] For instance: (*i*) the implementation in 1999 of important changes of the 1998 sixth comprehensive CPI revision (see Greenlees and Mason (1996) for more details), which included new housing sample and estimator, computer-assisted data collection for commodities and services sample, shift from area sample rotation to item category rotation using telephone Point-of-Purchase Survey, and redesigned Consumer Expenditure Survey processing system; (*ii*) the September 11, 2001, attack; (*iii*) the 2007–2009 Global Financial Crisis, and 2020-2023 COVID-19 pandemics; and (*iv*) changes in monetary policy due to zero lower bound on nominal interest rates, quantitative easing, negative long-run real interest rates.

CPI inflation rates up to month $(t-2)$. And, if month t is the pivot month (second month) of a quarter, the information set also contains current and past aggregate quarterly SPF backcasts/nowcasts/forecasts $\mathcal{F}_t\pi^{av}_{t+h}$, for $h \in \{-3, 0, 3, 6, 9, 12\}$. Since SPF forecasts are only available at a quarterly frequency, we use this frequency in our forecasting performance tests. Below, we detail how we build quarterly forecasts and their forecast errors.

After retrieving (logarithmized) filtered values of forecasted (logarithmized) average-price rates $E^*_t\pi^{av}_{t+h}$ and $E_{t-2}\pi^{av}_{t+h}$ for each pivot month t, we convert them back to annualized forecast levels:

$$\begin{aligned} \pi^{av^*}_{t,t+h} &\equiv \quad 100\left[\exp\left(4\tfrac{E^*_t\pi^{av}_{t+h}}{100}\right)-1\right] \\ \pi^{av}_{t-2,t+h} &\equiv \quad 100\left[\exp\left(4\tfrac{E_{t-2}\pi^{av}_{t+h}}{100}\right)-1\right] \end{aligned} \tag{8}$$

For simplicity, we talk about forecasts built with log-linearized relations $E^*_t\pi^{av}_{t+h} = E_{t-2}\pi^{av}_{t+h} + \mathfrak{s}^{av}_{h,t}$ and $E_{t-2}\pi^{av}_{t+h}$ when meaning $\pi^{av^*}_{t,t+h}$ and $\pi^{av}_{t-2,t+h}$.

In the effective testing window 2006:Q1 to 2023:Q2, we have 70 backcasts $\pi^{av^*}_{t,t-3}$ and $\pi^{av}_{t-2,t-3}$, 70 nowcasts $\pi^{av^*}_{t,t}$ and $\pi^{av}_{t-2,t}$, and $\left(70-\frac{h}{3}\right)$ forecasts $\pi^{av^*}_{t,t+h}$ and $\pi^{av}_{t-2,t+h}$ for each future horizon $h \in \{3, 6, 9, 12\}$. Since SPF forecasts are observed as quarterly logarithmized units in the model, annualized SPF forecasts are simply retrieved as $\pi^{spf}_{t,t+h} = 100\left[\exp\left(4\tfrac{\mathcal{F}_t\pi^{av}_{t+h}}{100}\right)-1\right]$.

Before computing forecast errors, we need to retrieve realized average-price rates $\pi^{av}_{r,t}$, where we use the subscript r to highlight realized observations. For that, we consider the final vintage of realized seasonally adjusted monthly CPI indices $P^{sa}_{r,t}$, available in July 2023, and compute realized average-prices $P^{av}_{r,t} = \frac{1}{3}\left(P^{sa}_{r,t+1} + P^{sa}_{r,t} + P^{sa}_{r,t-1}\right)$ and their quarterly rate $\pi^{av}_{r,t} = 100\left[\left(\frac{P^{av}_{r,t}}{P^{av}_{r,t-3}}\right)^4 - 1\right]$.

Lastly, we compute forecast errors as follows: (i) $\xi^{spf}_{t,t+h} = \pi^{spf}_{t,t+h} - \pi^{av}_{r,t+h}$ for SPF forecasts; (ii) $\xi^{av^*}_{t,t+h} = \pi^{av^*}_{t,t+h} - \pi^{av}_{r,t+h}$ for model-based best forecasts; and (iii) $\xi^{av}_{t-2,t+h} = \pi^{av}_{t-2,t+h} - \pi^{av}_{r,t+h}$ for model-based lagged forecasts.

For increasing-size sample windows, Table 2 shows forecast performance statistics for $\pi^{av^*}_{t,t+h}$ and $\pi^{av}_{t-2,t+h}$ relative to those of SPF. The first column shows SPF Mean Square Errors (MSE), i.e., $mean\left(\xi^{spf}_{t,t+h}\right)^2$, while the remaining columns depict the models' Relative Mean Square Errors (Relative MSE), i.e. $\frac{mean\left(\xi^{av^*}_{t,t+h}\right)^2}{mean\left(\xi^{spf}_{t,t+h}\right)^2}$ and $\frac{mean\left(\xi^{av}_{t-2,t+h}\right)^2}{mean\left(\xi^{spf}_{t,t+h}\right)^2}$. Table 3 shows the same results for 15-year fixed-size sample windows. The tables show p-values from both the Giacomini and White (2006) (GW) and Diebold and Mariano (1995) (DM) tests for predictive ability. Since the GW test is the most appropriate, as compared models are nested, significance stars reflect GW p-values. Ratios smaller than one imply that the models' forecasts are better than SPF forecasts. For the GW test,

we consider the conditional one. For the DM test, we use Newey-West covariance matrices and sample size correction.[20]

We draw four important lessons from the exercises: (i) nowcasts $(h = 0)$ performances, i.e. based on $E_t^*\pi_t^{av} = \left(E_{t-2}\pi_t^{av} + \mathfrak{s}_{0,t}^{av}\right)$, are strongly and significantly better than those from SPF; (ii) nowcasts's MSE's built with $E_{t-2}\pi_t^{av}$ are far from being as efficient as those obtained with $E_t^*\pi_t^{av}$; (iii) for backcasts $(h = -3)$, SPF dominates the model's forecasts $E_t^*\pi_{t-3}^{av}$; and (iv) for longer horizons $(h > 0)$, the model's forecasts $E_t^*\pi_{t+h}^{av}$ are at par with SPF survey.

As for the first lesson, nowcasts' MSEs (built with $E_t^*\pi_t^{av}$) are about 53%-57% of those obtained from SPF nowcasts. This outcome is important, for we do not add any extra and intra-quarter information, other than monthly nonseasonally adjusted CPI inflation and quarterly SPF forecasts. For comparison, Knotek II and Zaman (2017) find a similar nowcast Relative MSE in a monthly-frequency model, of about $\frac{1}{1.98} = 51\%$,[21] only after including a plethora of external higher-frequency information, meant to match the information set available to SPF responders. In addition to the monthly CPI inflation, the authors extract information from daily oil prices, weekly gasoline prices, and the history of monthly Personal Consumption Expenditure (PCE) rates. Here, we do not include external information other than that from past non-seasonally adjusted CPI inflation and current SPF forecasts.

As for the second lesson, i.e., regarding the finding that $E_{t-2}\pi_t^{av}$ are far from being as efficient as those obtained with $E_t^*\pi_t^{av} = \left(E_{t-2}\pi_t^{av} + \mathfrak{s}_{0,t}^{av}\right)$, it confirms our assumption that the latent component $\mathfrak{s}_{0,t}^{av}$, retrieved by Kalman filtering, does convey additional soft and intra-quarter information and contributes for forecast improvements. Since we obtain similar nowcast Relative MSE's as those obtained by Knotek II and Zaman (2017) using external data, it suggests the extra external higher-frequency information used by the authors is actually already embedded into the survey forecasts, and removing the effects of nowcast rigidity is enough for unveiling this purer information.

As for the third and fourth lessons, it implies that removing all forecast rigidity does not always allow for improved forecasts. In Section 5, we use a noisy-dispersed information model and obtain a theoretical result that explains those findings.

[20] The lag selection parameter L^* is based on Andrews and Monahan (1992): $L^* = floor\left(4\left(\frac{T}{100}\right)^{\frac{2}{9}}\right)$, where T is the sample size. As for the bandwidth value bm, we use $bm = 1 + L^*$.

[21] See third row of Table 7 in Knotek II and Zaman (2017).

Table 2: Forecast Performance - Increasing-Size Sample Windows

	MSE	Relative MSE for $\pi^{av^*}_{t,t+h}$						
h	SPF	RFR	SF_{-3}	SF_0	SF_3	SF_6	SF_9	SF_{12}
-3	0.300	1.000	$2.000^{\cdots}$	1.083	$1.129^{\cdots}$	$1.230^{\cdots}$	$1.230^{\cdots}$	$1.247^{\cdots}$
		–	p_{GW}=0.001	p_{GW}=0.145	p_{GW}=0.008	p_{GW}=0.006	p_{GW}=0.006	p_{GW}=0.006
		–	p_{DM}=0.000	p_{DM}=0.027	p_{DM}=0.000	p_{DM}=0.000	p_{DM}=0.000	p_{DM}=0.000
0	2.408	1.000	0.827^{***}	0.548^{***}	0.551^{**}	0.534^{***}	0.533^{***}	0.543^{***}
		–	p_{GW}=0.001	p_{GW}=0.005	p_{GW}=0.015	p_{GW}=0.010	p_{GW}=0.010	p_{GW}=0.010
		–	p_{DM}=0.008	p_{DM}=0.045	p_{DM}=0.049	p_{DM}=0.053	p_{DM}=0.053	p_{DM}=0.050
3	7.221	1.000	0.991	0.966	0.941	0.989	0.987	0.948
		–	p_{GW}=0.453	p_{GW}=0.324	p_{GW}=0.831	p_{GW}=0.912	p_{GW}=0.919	p_{GW}=0.868
		–	p_{DM}=0.362	p_{DM}=0.236	p_{DM}=0.628	p_{DM}=0.927	p_{DM}=0.915	p_{DM}=0.674
6	8.071	1.000	1.001	1.005	1.023	1.085	1.085	1.060
		–	p_{GW}=0.628	p_{GW}=0.153	p_{GW}=0.428	p_{GW}=0.291	p_{GW}=0.300	p_{GW}=0.450
		–	p_{DM}=0.839	p_{DM}=0.681	p_{DM}=0.665	p_{DM}=0.317	p_{DM}=0.316	p_{DM}=0.419
9	8.196	1.000	1.001	1.005	1.021	1.070	1.076	1.054
		–	p_{GW}=0.955	p_{GW}=0.857	p_{GW}=0.511	p_{GW}=0.337	p_{GW}=0.453	p_{GW}=0.361
		–	p_{DM}=0.893	p_{DM}=0.707	p_{DM}=0.674	p_{DM}=0.387	p_{DM}=0.365	p_{DM}=0.439
12	8.101	1.000	0.997	0.994	0.979	0.979	0.984	0.977^{*}
		–	p_{GW}=0.106	p_{GW}=0.113	p_{GW}=0.112	p_{GW}=0.136	p_{GW}=0.132	p_{GW}=0.096
		–	p_{DM}=0.298	p_{DM}=0.460	p_{DM}=0.591	p_{DM}=0.713	p_{DM}=0.762	p_{DM}=0.725

	MSE	Relative MSE for $\pi^{av}_{t-2,t+h}$						
h	SPF	RFR	SF_{-3}	SF_0	SF_3	SF_6	SF_9	SF_{12}
-3	0.300	0.967^{*}	$1.887^{\cdots}$	1.059	1.007	1.037	1.041	1.043
		p_{GW}=0.066	p_{GW}=0.002	p_{GW}=0.297	p_{GW}=0.932	p_{GW}=0.857	p_{GW}=0.790	p_{GW}=0.777
		p_{DM}=0.218	p_{DM}=0.000	p_{DM}=0.450	p_{DM}=0.960	p_{DM}=0.826	p_{DM}=0.808	p_{DM}=0.794
0	2.408	1.050	0.874^{***}	0.604^{***}	0.780	0.962^{*}	0.960^{*}	0.872
		p_{GW}=0.227	p_{GW}=0.002	p_{GW}=0.004	p_{GW}=0.153	p_{GW}=0.057	p_{GW}=0.059	p_{GW}=0.120
		p_{DM}=0.105	p_{DM}=0.003	p_{DM}=0.036	p_{DM}=0.163	p_{DM}=0.722	p_{DM}=0.718	p_{DM}=0.377
3	7.221	1.044	1.024	1.025	1.001	0.995	0.994	1.001
		p_{GW}=0.138	p_{GW}=0.167	p_{GW}=0.420	p_{GW}=0.298	p_{GW}=0.546	p_{GW}=0.505	p_{GW}=0.300
		p_{DM}=0.103	p_{DM}=0.070	p_{DM}=0.347	p_{DM}=0.996	p_{DM}=0.966	p_{DM}=0.962	p_{DM}=0.996
6	8.071	1.003	1.002	1.003	0.982	1.043	1.044	1.009
		p_{GW}=0.690	p_{GW}=0.297	p_{GW}=0.711	p_{GW}=0.464	p_{GW}=0.425	p_{GW}=0.418	p_{GW}=0.512
		p_{DM}=0.714	p_{DM}=0.847	p_{DM}=0.832	p_{DM}=0.827	p_{DM}=0.717	p_{DM}=0.718	p_{DM}=0.926
9	8.196	1.010	1.010	1.011	0.995	1.043	1.046	1.020
		p_{GW}=0.492	p_{GW}=0.333	p_{GW}=0.300	p_{GW}=0.312	p_{GW}=0.709	p_{GW}=0.649	p_{GW}=0.889
		p_{DM}=0.260	p_{DM}=0.225	p_{DM}=0.264	p_{DM}=0.907	p_{DM}=0.595	p_{DM}=0.578	p_{DM}=0.772
12	8.101	1.019	1.019	1.014	1.017	1.056	1.058	1.029
		p_{GW}=0.226	p_{GW}=0.156	p_{GW}=0.291	p_{GW}=0.593	p_{GW}=0.515	p_{GW}=0.523	p_{GW}=0.248
		p_{DM}=0.171	p_{DM}=0.161	p_{DM}=0.312	p_{DM}=0.521	p_{DM}=0.366	p_{DM}=0.341	p_{DM}=0.573

Notes: Increasing-Size Sample Windows. First sample: Jan. 1991 to Dec. 2005. Last sample: Jan. 1991 to Dec. 2022. Quarterly testing window: 2006:Q1 to 2023:Q2. Relative Mean Square Errors (Relative MSE) are $\frac{mean\left(\xi^{av^*}_{t,t+h}\right)^2}{mean\left(\xi^{spf}_{t,t+h}\right)^2}$ *and* $\frac{mean\left(\xi^{av}_{t-2,t+h}\right)^2}{mean\left(\xi^{spf}_{t,t+h}\right)^2}$*, and p-values are from both the unconditional Giacomini and White (2006) (GW) and Diebold and Mariano (1995) (DM) tests for predictive ability. Ratios smaller than one imply that models' forecasts are better than SPF forecasts. Significance notation: 1% (***), 5% (**) and 10% (*) for ratios smaller than unity, and 1% (···), 5% (··) and 10% (·) for ratios larger than unity.*

Table 3: Forecast Performance - 15-Year Fixed-Size Sample Windows

	MSE	Relative MSE for $\pi^{av^*}_{t,t+h}$						
h	SPF	RFR	SF_{-3}	SF_0	SF_3	SF_6	SF_9	SF_{12}
-3	0.300	1.000	$2.180^{\cdots}$	$1.183^{\cdot\cdot}$	$1.160^{\cdots}$	$1.255^{\cdots}$	$1.227^{\cdots}$	$1.261^{\cdots}$
		–	p_{GW}=0.001	p_{GW}=0.028	p_{GW}=0.006	p_{GW}=0.003	p_{GW}=0.006	p_{GW}=0.004
		–	p_{DM}=0.000	p_{DM}=0.003	p_{DM}=0.000	p_{DM}=0.000	p_{DM}=0.000	p_{DM}=0.000
0	2.408	1.000	0.801^{***}	0.572^{***}	0.563^{**}	0.578^{**}	0.542^{***}	0.558^{**}
		–	p_{GW}=0.000	p_{GW}=0.002	p_{GW}=0.016	p_{GW}=0.013	p_{GW}=0.010	p_{GW}=0.012
		–	p_{DM}=0.016	p_{DM}=0.043	p_{DM}=0.050	p_{DM}=0.048	p_{DM}=0.055	p_{DM}=0.052
3	7.221	1.000	0.985	0.971	0.951	0.958	0.968	0.952
		–	p_{GW}=0.154	p_{GW}=0.339	p_{GW}=0.832	p_{GW}=0.873	p_{GW}=0.940	p_{GW}=0.897
		–	p_{DM}=0.245	p_{DM}=0.238	p_{DM}=0.700	p_{DM}=0.741	p_{DM}=0.799	p_{DM}=0.705
6	8.071	1.000	0.998	1.006	1.019	1.077	1.123	1.102
		–	p_{GW}=0.272	p_{GW}=0.156	p_{GW}=0.443	p_{GW}=0.461	p_{GW}=0.324	p_{GW}=0.440
		–	p_{DM}=0.758	p_{DM}=0.629	p_{DM}=0.713	p_{DM}=0.357	p_{DM}=0.245	p_{DM}=0.303
9	8.196	1.000	0.999	1.005	1.016	1.059	1.079	1.052
		–	p_{GW}=0.862	p_{GW}=0.835	p_{GW}=0.481	p_{GW}=0.142	p_{GW}=0.360	p_{GW}=0.295
		–	p_{DM}=0.884	p_{DM}=0.682	p_{DM}=0.744	p_{DM}=0.441	p_{DM}=0.361	p_{DM}=0.462
12	8.101	1.000	0.995	0.995	0.984	1.064	1.068	1.077
		–	p_{GW}=0.146	p_{GW}=0.112	p_{GW}=0.120	p_{GW}=0.643	p_{GW}=0.530	p_{GW}=0.525
		–	p_{DM}=0.262	p_{DM}=0.519	p_{DM}=0.678	p_{DM}=0.328	p_{DM}=0.233	p_{DM}=0.240

	MSE	Relative MSE for $\pi^{av}_{t-2,t+h}$						
h	SPF	RFR	SF_{-3}	SF_0	SF_3	SF_6	SF_9	SF_{12}
-3	0.300	0.960^{*}	$2.068^{\cdots}$	$1.178^{\cdot\cdot}$	1.031	1.014	1.041	1.043
		p_{GW}=0.059	p_{GW}=0.001	p_{GW}=0.034	p_{GW}=0.912	p_{GW}=0.997	p_{GW}=0.979	p_{GW}=0.968
		p_{DM}=0.184	p_{DM}=0.001	p_{DM}=0.033	p_{DM}=0.824	p_{DM}=0.921	p_{DM}=0.797	p_{DM}=0.786
0	2.408	1.050	0.845^{***}	0.621^{***}	0.763	0.924	0.960^{*}	0.916
		p_{GW}=0.183	p_{GW}=0.000	p_{GW}=0.002	p_{GW}=0.112	p_{GW}=0.113	p_{GW}=0.059	p_{GW}=0.108
		p_{DM}=0.086	p_{DM}=0.015	p_{DM}=0.034	p_{DM}=0.149	p_{DM}=0.647	p_{DM}=0.895	p_{DM}=0.624
3	7.221	$1.051^{\cdot}$	1.015	1.021	0.999	1.023	0.994	1.022
		p_{GW}=0.094	p_{GW}=0.335	p_{GW}=0.139	p_{GW}=0.162	p_{GW}=0.266	p_{GW}=0.505	p_{GW}=0.390
		p_{DM}=0.075	p_{DM}=0.298	p_{DM}=0.422	p_{DM}=0.996	p_{DM}=0.834	p_{DM}=0.946	p_{DM}=0.846
6	8.071	1.009	0.998	1.002	0.976	0.989	1.044	1.010
		p_{GW}=0.790	p_{GW}=0.230	p_{GW}=0.971	p_{GW}=0.549	p_{GW}=0.822	p_{GW}=0.418	p_{GW}=0.644
		p_{DM}=0.511	p_{DM}=0.853	p_{DM}=0.878	p_{DM}=0.725	p_{DM}=0.896	p_{DM}=0.696	p_{DM}=0.918
9	8.196	1.014	1.014	1.017	1.001	0.995	1.046	1.013
		p_{GW}=0.499	p_{GW}=0.367	p_{GW}=0.262	p_{GW}=0.167	p_{GW}=0.995	p_{GW}=0.649	p_{GW}=0.831
		p_{DM}=0.277	p_{DM}=0.248	p_{DM}=0.214	p_{DM}=0.968	p_{DM}=0.932	p_{DM}=0.636	p_{DM}=0.837
12	8.101	1.020	1.023	1.020	1.041	1.024	1.058	1.020
		p_{GW}=0.215	p_{GW}=0.195	p_{GW}=0.213	p_{GW}=0.242	p_{GW}=0.605	p_{GW}=0.523	p_{GW}=0.428
		p_{DM}=0.170	p_{DM}=0.150	p_{DM}=0.208	p_{DM}=0.215	p_{DM}=0.638	p_{DM}=0.560	p_{DM}=0.672

Notes: 15-Year Fixed-Size Sample Windows. First sample: Jan. 1991 to Dec. 2005. Last sample: Jan. 2008 to Dec. 2022. Quarterly testing window: 2006:Q1 to 2023:Q2. Relative Mean Square Errors (Relative MSE) are $\frac{mean\left(\xi^{av^*}_{t,t+h}\right)^2}{mean\left(\xi^{spf}_{t,t+h}\right)^2}$ *and* $\frac{mean\left(\xi^{av}_{t-2,t+h}\right)^2}{mean\left(\xi^{spf}_{t,t+h}\right)^2}$*, and p-values are from both the unconditional Giacomini and White (2006) (GW) and Diebold and Mariano (1995) (DM) tests for predictive ability. Ratios smaller than one imply that models' forecasts are better than SPF forecasts. Significance notation: 1% (***), 5% (**) and 10% (*) for ratios smaller than unity, and 1% (···), 5% (··) and 10% (·) for ratios larger than unity.*

5 Resetting Forecast Dominance

As shown in Section 4, Resetting Nowcasts strongly dominate SPF Average Nowcasts for SPF, but Resetting Forecasts are only just as good for longer horizons. Therefore, it begs the question, *which are the conditions for Resetting Forecasts to dominate Average Forecasts?*

In this section, for simplicity, we answer this question by considering a model with noisy-dispersed information. A more general hybrid formulation with noisy-dispersed and sticky information (e.g. Andrade and Le Bihan (2013) and Areosa et al. (2020)) would only add complexity without changing much of the main lessons. For proof of concept purposes, we consider the quarterly frequency and assume a simple data-generating process (DGP) for the average price rate.

5.1 Noisy-Dispersed Forecasts

We slightly depart from Coibion and Gorodnichenko (2015) by extending the model to allow for disagreement and horizon-specific parameters. Assume each respondent $i \in [0,1]$ initially builds raw forecasts $E^*_{i,q}\pi^{av}_{q+\mathfrak{h}}$, for each quarterly horizon $\mathfrak{h} \in \{-1,0,1,2,3,4\}$. Being subject to noisy information, her initial raw forecast satisfies $E^*_{i,q}\pi^{av}_{q+\mathfrak{h}} = \pi^{av}_{q+\mathfrak{h}} + \upsilon_{i,\mathfrak{h},q+\mathfrak{h}}$, where $\upsilon_{i,\mathfrak{h},q+\mathfrak{h}} \sim N\left(0, \sigma^2_{\upsilon,\mathfrak{h}}\right)$ is the individual forecast error for horizon $\mathfrak{h}$. Notice the variance $\sigma^2_{\upsilon,\mathfrak{h}}$ might be horizon-specific.

Unbeknownst to each forecaster, the forecast error is comprised of a common public noise $\eta_{\mathfrak{h},q+\mathfrak{h}} \sim N\left(0, \sigma^2_{\eta,\mathfrak{h}}\right)$ and a private component $\delta_{i,\mathfrak{h},q+\mathfrak{h}} \sim N\left(0, \sigma^2_{\delta,\mathfrak{h}}\right)$, i.e. $\upsilon_{i,\mathfrak{h},q+\mathfrak{h}} \equiv (\eta_{\mathfrak{h},q+\mathfrak{h}} + \delta_{i,\mathfrak{h},q+\mathfrak{h}})$, where $\delta_{i,\mathfrak{h},q+\mathfrak{h}}$ captures dispersion across all individuals, i.e. $\int_0^1 \delta_{i,\mathfrak{h},q+\mathfrak{h}} di = 0$. It implies $\sigma^2_{\upsilon,\mathfrak{h}} \equiv \left(\sigma^2_{\eta,\mathfrak{h}} + \sigma^2_{\delta,\mathfrak{h}}\right)$ and $\int_0^1 \upsilon_{i,\mathfrak{h},q+\mathfrak{h}} di = \eta_{\mathfrak{h},q+\mathfrak{h}}$.

Under certain conditions, Direct Multistep (DMS) models[22] – or direct forecasts – outperform Iterated Multistep (IMS) models in forecasting, and might be robust to model misspecification (e.g. Marcellino et al. (2006) and McCracken and McGillicuddy (2018), among others). Since the DMS models' forecast errors are horizon-specific, no iteration is required for producing forecasts. In particular, McCracken and McGillicuddy (2018) find evidence that DMS models are better for forecasting nominal variables such as prices, wages, and money.

Therefore, forecasters would have incentives to use DMS models when producing their initial raw forecasts $E^*_{i,q}\pi^{av}_{q+\mathfrak{h}}$, retrieved after estimating equations like $\pi^{av}_{q+\mathfrak{h}} = (\rho_{\mathfrak{h}})^{\mathfrak{h}+1}\, \pi^{av}_{q-1} + \xi_{\mathfrak{h},q+\mathfrak{h}}$, where $|\rho_{\mathfrak{h}}| < 1$ and $\xi_{\mathfrak{h},q+\mathfrak{h}} \sim N\left(0, \sigma^2_{\xi,\mathfrak{h}}\right)$ for each horizon. Direct forecasting is equivalent to assuming horizon-specific DGP processes for inflation, each one aimed at producing recursive forecasts for

[22] Direct Multistep models can be view as the foundation of Local Projection methods (e.g. Jorda (2005) and Jorda (2023)).

each specific horizon $\mathfrak{h}$: $\pi_q^{av} = \rho_{\mathfrak{h}}\pi_{q-1}^{av} + \varepsilon_{\mathfrak{h},q}$, where $\varepsilon_{\mathfrak{h},q} \sim N\left(0, \sigma_{\mathfrak{h}}^2\right)$. Note that, no matter the quarterly forecasting horizon $\mathfrak{h}$ and values for parameters for $\rho_{\mathfrak{h}}$, $\sigma_{\varepsilon,\mathfrak{h}}^2$ and $\sigma_{\xi,\mathfrak{h}}^2$, the implied ergodic distribution for π_q^{av} must be the same. That is, if $\bar{\sigma}^2 \equiv var\left(\pi_q^{av}\right)$ is its ergodic variance, the horizon-specific parameters must satisfy $\bar{\sigma}^2 = \frac{\sigma_{\mathfrak{h}}^2}{\left(1-(\rho_{\mathfrak{h}})^2\right)} = \frac{\sigma_{\xi,\mathfrak{h}}^2}{\left(1-(\rho_{\mathfrak{h}})^{2(\mathfrak{h}+1)}\right)}$.

Each forecaster is aware of its signal $E_{i,q}^*\pi_{q+\mathfrak{h}}^{av} = \pi_{q+\mathfrak{h}}^{av} + \upsilon_{i,\mathfrak{h},q+\mathfrak{h}}$ and state $\pi_q^{av} = \rho_{\mathfrak{h}}\pi_{q-1}^{av} + \varepsilon_{\mathfrak{h},q}$ equations. In addition, at each quarter q, she observes $E_{i,q}^*\pi_{q+\mathfrak{h}}^{av}$ and past values of realized inflation π_{q-k}^{av}, for $k = \{1, 2, ...\}$. Using Kalman filtering, she can improve[23] her initial raw forecast $E_{i,q}^*\pi_{q+\mathfrak{h}}^{av}$ into $\mathcal{F}_{i,q}\pi_{q+\mathfrak{h}}^{av} \equiv E\left(\pi_{q+\mathfrak{h}}^{av} | E_{i,q}^*\pi_{q+\mathfrak{h}}^{av}, \left\{\pi_{q-\tau}^{av}\right\}_{\tau\geq 1}\right)$. Kalman recursion delivers:

$$\mathcal{F}_{i,q}\pi_{q+\mathfrak{h}}^{av} = (1-\gamma_{\mathfrak{h}})\,\mathcal{F}_{i,q-1}\pi_{q+\mathfrak{h}}^{av} + \gamma_{\mathfrak{h}}E_{i,q}^*\pi_{q+\mathfrak{h}}^{av} \tag{9}$$

where $\gamma_{\mathfrak{h}} = \frac{\kappa_{\mathfrak{h}}\bar{\sigma}^2}{\kappa_{\mathfrak{h}}\bar{\sigma}^2+\sigma_{\upsilon,\mathfrak{h}}^2}$ is the horizon-specific Kalman gain, the inertia-based adjustment factor[24] is $\kappa_{\mathfrak{h}} = \frac{\left(1-(\rho_{\mathfrak{h}})^2\right)}{2}\left[\left(1-\frac{\sigma_{\upsilon,\mathfrak{h}}^2}{\bar{\sigma}^2}\right) + \sqrt{\left(1-\frac{\sigma_{\upsilon,\mathfrak{h}}^2}{\bar{\sigma}^2}\right)^2 + \frac{4}{\left(1-(\rho_{\mathfrak{h}})^2\right)}\frac{\sigma_{\upsilon,\mathfrak{h}}^2}{\bar{\sigma}^2}}\right]$, and $\bar{\sigma}^2 = \frac{\sigma_{\mathfrak{h}}^2}{\left(1-(\rho_{\mathfrak{h}})^2\right)}$ is the unconditional variance. Note the reasons leading to horizon-specific Kalman gains $\gamma_{\mathfrak{h}}$ are direct forecasting and horizon-specific error variances.

In turn, the Average Forecast $\mathcal{F}_q\pi_{q+\mathfrak{h}}^{av} \equiv \int_0^1 \mathcal{F}_{i,q}\pi_{q+\mathfrak{h}}^{av}di$ evolves according to

$$\mathcal{F}_q\pi_{q+\mathfrak{h}}^{av} = (1-\gamma_{\mathfrak{h}})\,\mathcal{F}_{q-1}\pi_{q+\mathfrak{h}}^{av} + \gamma_{\mathfrak{h}}E_q^*\pi_{q+\mathfrak{h}}^{av} \tag{10}$$

where $E_q^*\pi_{q+\mathfrak{h}}^{av} = \int_0^1 E_{i,q}^*\pi_{q+\mathfrak{h}}^{av}di = \pi_{q+\mathfrak{h}}^{av} + \eta_{\mathfrak{h},q+\mathfrak{h}}$ is the Resetting Forecast, not observed by any individual forecaster when providing SPF with $\mathcal{F}_{i,q}\pi_{q+\mathfrak{h}}^{av}$.

Therefore, as shown in Andrade and Le Bihan (2013) and Coibion and Gorodnichenko (2015), the forecast rigidity parameters defined in Section 2.2.3 have a one-to-one mapping into those Kalman gains, i.e. $\alpha_{\mathfrak{h}} = (1-\gamma_{\mathfrak{h}})$.

5.2 Forecast Dominance

Kalman recursion applied to this model implies $\mathcal{F}_{i,q}\pi_{q+1+\mathfrak{h}}^{av} = \rho_{\mathfrak{h}}\mathcal{F}_{i,q}\pi_{q+\mathfrak{h}}^{av}$ and $\mathcal{F}_q\pi_{q+1+\mathfrak{h}}^{av} = \rho_{\mathfrak{h}}\mathcal{F}_q\pi_{q+\mathfrak{h}}^{av}$. Therefore, using (9) and (10) as in Appendix A, the Individual Forecast error $\xi_{i,q,\mathfrak{h}} \equiv \mathcal{F}_{i,q}\pi_{q+\mathfrak{h}}^{av} - \pi_{q+\mathfrak{h}}^{av}$, Average Forecast error $\xi_{q,\mathfrak{h}} \equiv \int_0^1 \xi_{i,q,\mathfrak{h}}di = \mathcal{F}_q\pi_{q+\mathfrak{h}}^{av} - \pi_{q+\mathfrak{h}}^{av}$, and Resetting Forecast error $\xi_{q,\mathfrak{h}}^* \equiv$

[23] Given her initial raw forecast $E_{i,q}^*\pi_{q+\mathfrak{h}}^{av} = \pi_{q+\mathfrak{h}}^{av} + \upsilon_{i,\mathfrak{h},q+\mathfrak{h}}$, Kalman filtering leading to $\mathcal{F}_{i,q}^*\pi_{q+\mathfrak{h}}^{av}$ always minimizes the variance of her own forecast errors.

[24] As usual, $\kappa_{\mathfrak{h}} = 1$ if $\rho_{\mathfrak{h}} = 0$.

$E_q^* \pi_{q+\mathfrak{h}}^{av} - \pi_{q+\mathfrak{h}}^{av}$ evolve according to the following dynamics:

$$\begin{aligned}
\xi_{i,q,\mathfrak{h}} &= (1-\gamma_{\mathfrak{h}})\,\rho_{\mathfrak{h}}\xi_{i,q-1,\mathfrak{h}} - (1-\gamma_{\mathfrak{h}})\,\varepsilon_{\mathfrak{h},q+\mathfrak{h}} + \gamma_{\mathfrak{h}}\upsilon_{i,\mathfrak{h},q+\mathfrak{h}} \\
\xi_{q,\mathfrak{h}} &= (1-\gamma_{\mathfrak{h}})\,\rho_{\mathfrak{h}}\xi_{q-1,\mathfrak{h}} - (1-\gamma_{\mathfrak{h}})\,\varepsilon_{\mathfrak{h},q+\mathfrak{h}} + \gamma_{\mathfrak{h}}\eta_{\mathfrak{h},q+\mathfrak{h}} \\
\xi_{q,\mathfrak{h}}^* &= \eta_{\mathfrak{h},q+\mathfrak{h}}
\end{aligned}$$

It implies that their unconditional variances $\vartheta_{i,\mathfrak{h}} \equiv var\left(\xi_{i,q,\mathfrak{h}}\right)$, $\vartheta_{\mathfrak{h}} \equiv var\left(\xi_{q,\mathfrak{h}}\right)$, and $\vartheta_{\mathfrak{h}}^* \equiv var\left(\xi_{q,\mathfrak{h}}^*\right)$ are:

$$\vartheta_{i,\mathfrak{h}} = \frac{\left(1-\gamma_{\mathfrak{h}}\right)^2\sigma_{\mathfrak{h}}^2+\left(\gamma_{\mathfrak{h}}\right)^2\sigma_{\upsilon,\mathfrak{h}}^2}{1-\left(1-\gamma_{\mathfrak{h}}\right)^2\rho_{\mathfrak{h}}^2} \quad ; \; \vartheta_{\mathfrak{h}} = \frac{\left(1-\gamma_{\mathfrak{h}}\right)^2\sigma_{\mathfrak{h}}^2+\left(\gamma_{\mathfrak{h}}\right)^2\sigma_{\eta,\mathfrak{h}}^2}{1-\left(1-\gamma_{\mathfrak{h}}\right)^2\rho_{\mathfrak{h}}^2} \quad ; \; \vartheta_{\mathfrak{h}}^* = \sigma_{\eta,\mathfrak{h}}^2 \tag{11}$$

where again $\upsilon_{i,\mathfrak{h},q+\mathfrak{h}} \equiv (\eta_{\mathfrak{h},q+\mathfrak{h}} + \delta_{i,\mathfrak{h},q+\mathfrak{h}})$ and $\sigma_{\upsilon,\mathfrak{h}}^2 \equiv \left(\sigma_{\eta,\mathfrak{h}}^2 + \sigma_{\delta,\mathfrak{h}}^2\right)$.

It is easy to verify that $\vartheta_{i,\mathfrak{h}} \geq \vartheta_{\mathfrak{h}}$. That is, $\vartheta_{i,\mathfrak{h}}$ also accounts for the extra effect of disagreement on top of the variance $\vartheta_{\mathfrak{h}}$ of the Average Forecast error. Therefore, the ratio $\frac{\vartheta_{i,\mathfrak{h}}}{\vartheta_{\mathfrak{h}}} \geq 1$ is an appropriate measure of disagreement.

Since the Resetting Forecast $E_q^* \pi_{q+\mathfrak{h}}^{av}$ and the Average Forecast $\mathcal{F}_q \pi_{q+\mathfrak{h}}^{av} = \int_0^1 \mathcal{F}_{i,q} \pi_{q+\mathfrak{h}}^{av}$ are not biased, forecasting dominance is equivalent to having the smallest variance of forecast errors. Therefore, knowing estimates for the DGP parameters $\left(\rho_{\mathfrak{h}}, \bar{\sigma}^2\right)$, rigidity parameters $\gamma_{\mathfrak{h}}$, and noise variances $\left(\sigma_{\upsilon,\mathfrak{h}}^2, \sigma_{\eta,\mathfrak{h}}^2\right)$ is enough for telling whether the Resetting Forecast dominates the Average Forecast, i.e. if $\vartheta_{q,\mathfrak{h}}^* < \vartheta_{q,\mathfrak{h}}$.

However, estimates for the noise variances $\left(\sigma_{\upsilon,\mathfrak{h}}^2, \sigma_{\eta,\mathfrak{h}}^2\right)$ are not readily obtainable from survey microdata, as forecasters only reveal values for $\mathcal{F}_{i,q}\pi_{q+\mathfrak{h}}^{av}$ and not their initial raw forecasts $E_{i,q}^* \pi_{q+\mathfrak{h}}^{av}$. Therefore, even though the econometrician estimates $\vartheta_{q,\mathfrak{h}}$, she cannot infer $\vartheta_{q,\mathfrak{h}}^* = \sigma_{\eta,\mathfrak{h}}^2$.

For coping with this issue, only using statistics easily obtainable from the time series of CPI inflation and SPF microdata of individual forecasts, the following proposition provides an equivalent condition to verify whether Resetting Forecasts dominate Average Forecasts. More specifically, a few sufficient statistics, i.e. $\vartheta_{i,\mathfrak{h}}$, $\vartheta_{\mathfrak{h}}$ and $\bar{\sigma}^2$, are enough to verify dominance. And estimates of those variances are very easy to obtain from the realized quarterly average price rates of CPI inflation and SPF microdata.

The basic message of the proposition is that Resetting Forecasts dominate Average Forecasts when disagreement is sufficiently large, but not excessively large, so that forecast efficiency is compromised. For reasons better explained further on, we call the conditions leading to the disagreement lower and upper bounds as the *harmonic* and *efficiency conditions*.

Proposition 2 *Consider the modelling assumptions and results presented in Sections 5.1 and 5.2. In this case, the Resetting Forecast* $E_q^* \pi_{q+\mathfrak{h}}^{av}$ *has better forecasting performance than the Average Forecast* $\mathcal{F}_q \pi_{q+\mathfrak{h}}^{av}$ *if and only if disagreement* $\frac{\vartheta_{i,\mathfrak{h}}}{\vartheta_{\mathfrak{h}}}$ *satisfies the following condition:*

$$\frac{2}{\left[1+(\bar{\sigma}^2/\vartheta_{\mathfrak{h}})^{-1}\right]} < \frac{\vartheta_{i,\mathfrak{h}}}{\vartheta_{\mathfrak{h}}} < \frac{\bar{\sigma}^2}{\vartheta_{\mathfrak{h}}} \tag{12}$$

The proof is shown in Appendix A.

The right-hand inequality $\frac{\vartheta_{i,\mathfrak{h}}}{\vartheta_{\mathfrak{h}}} < \frac{\bar{\sigma}^2}{\vartheta_{\mathfrak{h}}}$ has the intuition of an *efficiency condition*, as the variance of Individual Forecast errors $\vartheta_{i,\mathfrak{h}}$ should be smaller than the unconditional variance of inflation $\bar{\sigma}^2$. Otherwise, individuals would be better off by simply using the inflation unconditional mean as their forecast. The left-hand inequality $\frac{2}{\left[1+(\bar{\sigma}^2/\vartheta_{\mathfrak{h}})^{-1}\right]} < \frac{\vartheta_{i,\mathfrak{h}}}{\vartheta_{\mathfrak{h}}}$ is the *harmonic condition*, as it states that disagreement $\frac{\vartheta_{i,\mathfrak{h}}}{\vartheta_{\mathfrak{h}}}$ should be larger than the harmonic mean between unity and the efficiency limit $\frac{\bar{\sigma}^2}{\vartheta_{\mathfrak{h}}}$.

Note that, if there is no disagreement (i.e. $\frac{\vartheta_{i,\mathfrak{h}}}{\vartheta_{\mathfrak{h}}} = 1$), the Resetting Forecast never dominates the Average Forecast. Otherwise, there will be an analytical contradiction, for the efficiency condition implies $\vartheta_{\mathfrak{h}} < \bar{\sigma}^2$, while the harmonic condition implies the opposite, i.e., $\vartheta_{\mathfrak{h}} > \bar{\sigma}^2$.

5.2.1 Testing Theoretical Forecast Dominance

We highlight the result (12) is obtained using a simplified DGP process for inflation, and assuming forecasts are unbiased, and the main friction governing forecasts formation comes from noisy-dispersed information. Nonetheless, Proposition 2 can be used as a fast way to suggest the horizons in which the Resetting Forecast dominate the Aggregate Forecasts before estimating the forecast model and formally testing its forecast performance, as carried out in Sections 3.1 and 4. Using result (12), all we need to verify the dominance are three variance estimates, easily recovered from CPI average price rates and the microdata of SPF individual forecasts: (*i*) sample variance of Individual Forecast errors $\hat{\vartheta}_{i,\mathfrak{h}}$; (*ii*) sample variance of Average Forecast errors $\hat{\vartheta}_{\mathfrak{h}}$; and (*iii*) sample variance of CPI average price rates $\widehat{\bar{\sigma}}^2$. Here, hatted parameters indicate sample estimates.

Therefore, in this section, we test whether the result (12) can provide us with the same message that we obtained in Section 4, in terms of informing us of the horizons in which Resetting Forecasts dominates Average Forecasts. By construction, result (12) does not tell us how strong forecast dominance is, but rather serves as an indication of whether there is forecast dominance. Since the sample variances $\hat{\vartheta}_{i,\mathfrak{h}}$, $\hat{\vartheta}_{\mathfrak{h}}$, and $\widehat{\bar{\sigma}}^2$ are not used in the exercises shown in Sections 3.1 and 4, the

analyses carried out with (12) are independent of those shown in the previous sections.

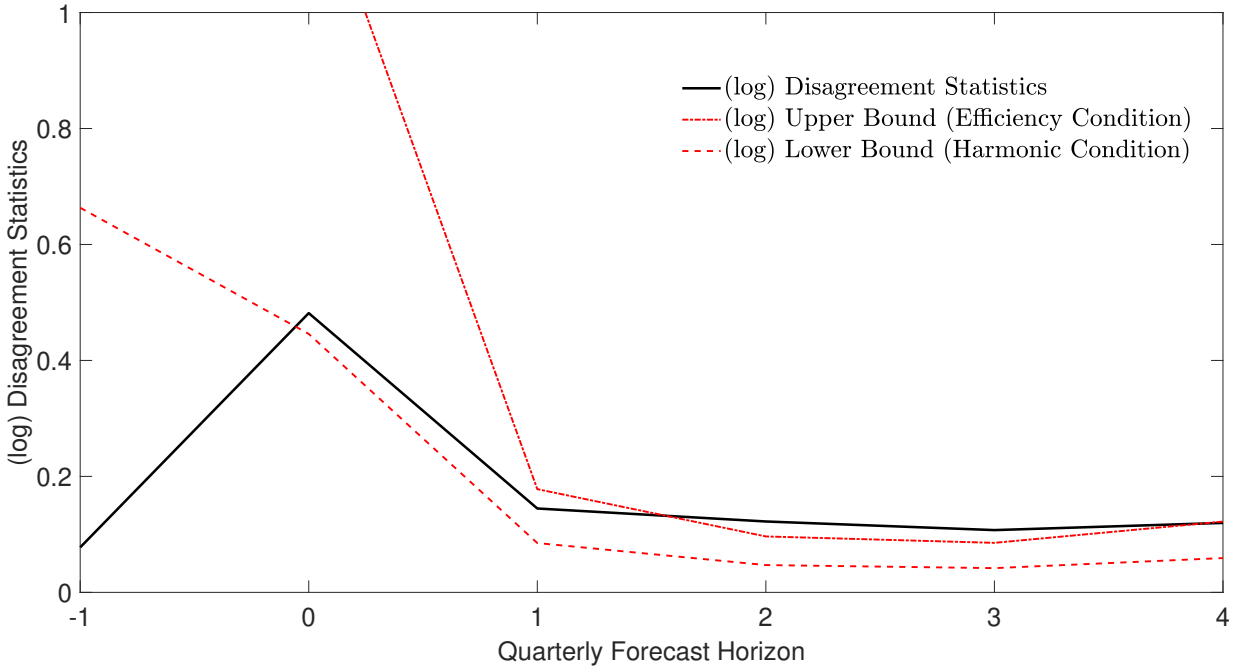


Figure 4: Forecast Dominance Implied by Disagreement

Notes: Forecast Performance Exercise based on Proposition 2, using disagreement metrics from microdata of SPF individual forecasts for CPI inflation.

Figure 4 draws the (log) disagreement statistics $\frac{\hat{\vartheta}_{i,\mathfrak{h}}}{\hat{\vartheta}_{\mathfrak{h}}}$ along with the (log) upper and lower bounds implied by the efficiency and disagreement conditions defined in (12). The sample variances are retrieved from CPI average price rates and the microdata of SPF individual forecasts, using the same effective testing window used in Section 4: 2006:Q1 to 2023:Q2. Since results (9), (11) and (12) are obtained under the assumption that forecasts are unbiased, we demeaned the individual forecasts errors before computing the statistics.[25]

Note the conclusions are in line with the Relative MSE's for $\pi^{av^*}_{t,t+h}$, shown in Tables **??** to 3 in Section 4, especially in exercises with unrestricted models. That is, Resetting Forecasts errors have smaller variances for nowcasts ($\mathfrak{h} = 0$), 1-quarter ahead forecasts ($\mathfrak{h} = 1$) and 4-quarter ahead forecasts ($\mathfrak{h} = 4$), as disagreement $\frac{\hat{\vartheta}_{i,\mathfrak{h}}}{\hat{\vartheta}_{\mathfrak{h}}}$ lies inside the theoretical interval. For 2-quarter and 3-quarter ahead forecasts, disagreement is located slightly above the interval upper bound, whereas it lies well below the interval lower bound for backcasts.

[25] Allowing for biased forecasts require adjusting those three systems, without changing much the analytical and empirical results we obtain.

6 Conclusions

Professional inflation forecasts contain valuable information obscured by information frictions that vary systematically across forecast horizons. By explicitly modeling these horizon-specific frictions, we extract improved forecasts that significantly outperform Survey of Professional Forecasters consensus nowcasts while matching performance at longer horizons.

Our results establish three main findings. First, forecast rigidity increases sharply with horizon length, rising from essentially zero for backcasts to 0.81 beyond two quarters. Models imposing either rational expectations or uniform rigidity across horizons are strongly rejected and fail to improve upon survey averages. Second, accounting for this heterogeneity yields substantial gains: our Resetting Nowcasts reduce mean squared errors by 50 percent relative to SPF averages in pseudo-real-time tests. Third, we provide a tractable theoretical framework that predicts when such improvements will emerge based on three sufficient statistics computed from survey microdata.

The theoretical criterion reveals that improved forecasts dominate when disagreement among individual forecasters lies within an optimal interval—large enough to signal meaningful information dispersion but not so large that forecasts become unreliable. Applied to SPF data, these microdata-based bounds correctly predict the horizons where our approach succeeds, suggesting the method generalizes readily to other surveys and variables.

Our inflation decomposition also offers policy-relevant insights. The 2021-2023 inflation surge primarily reflected medium-run transitory components rather than permanent shifts in trend inflation, with implications for appropriate monetary policy responses.

These findings open several avenues for future research. First, extending the framework to incorporate real-time data flow and forecast updates could further enhance nowcasting performance. Second, applying the approach to other macroeconomic variables—such as GDP growth, unemployment, or financial market indicators—would test the method's broader applicability. Third, investigating whether combining our Resetting Forecasts with machine learning techniques or high-frequency data could yield additional gains remains an open question. Finally, understanding how forecast frictions evolve during periods of structural change or regime shifts could improve real-time policy analysis during economic turbulence.

The practical value of our approach lies in its simplicity and generalizability. Policymakers and forecasters can use readily available survey microdata to identify which forecast horizons offer the greatest potential for improvement before investing in more elaborate modeling efforts. This provides a cost-effective screening tool for allocating resources toward the most promising forecasting

enhancements across different variables and time horizons.

References

Aiolfi, M., Capistran, C., Timmermann, A., 2012. Forecast Combinations, in: The Oxford Handbook of Economic Forecasting. 1 ed.. Oxford University Press, pp. 355–388.

Andrade, P., Crump, R.K., Eusepi, S., Moench, E., 2016. Fundamental disagreement. Journal of Monetary Economics 83, 106–128.

Andrade, P., Le Bihan, H., 2013. Inattentive professional forecasters. Journal of Monetary Economics 60, 967–982.

Andrews, D.W.K., Monahan, J.C., 1992. An Improved Heteroskedasticity and Autocorrelation Consistent Covariance Matrix Estimator. Econometrica 60, 953–966.

Ang, A., Bekaert, G., Wei, M., 2007. Do macro variables, asset markets, or surveys forecast inflation better? Journal of Monetary Economics 54, 1163–1212.

Areosa, M.B.M., Areosa, W.D., Carrasco, V., 2020. A sticky-dispersed information Phillips Curve: a model with partial and delayed information. Macroeconomic Dynamics 24, 747–773.

Beveridge, S., Nelson, C.R., 1981. A new approach to decomposition of economic time series into permanent and transitory components with particular attention to measurement of the 'business cycle'. Journal of Monetary Economics 7, 151–174.

Capistran, C., Timmermann, A., 2009a. Disagreement and Biases in Inflation Expectations. Journal of Money, Credit and Banking 41, 365–396.

Capistran, C., Timmermann, A., 2009b. Forecast Combination With Entry and Exit of Experts. Journal of Business & Economic Statistics 27, 428–440.

Cogley, T., Sbordone, A.M., 2008. Trend Inflation, Indexation, and Inflation Persistence in the New Keynesian Phillips Curve. American Economic Review 98, 2101–2126.

Coibion, O., Gorodnichenko, Y., 2012. What Can Survey Forecasts Tell Us about Information Rigidities? Journal of Political Economy 120, 116–159.

Coibion, O., Gorodnichenko, Y., 2015. Information Rigidity and the Expectations Formation Process: A Simple Framework and New Facts. American Economic Review 105, 2644–2678.

Croushore, D., 2010. An Evaluation of Inflation Forecasts from Surveys Using Real-Time Data. The B.E. Journal of Macroeconomics 10.

Croushore, D., Stark, T., 2019. Fifty Years of the Survey of Professional Forecasters. Economic Insights, Federal Reserve Bank of Philadelphia 4.

Crump, R.K., Eusepi, S., Lucca, D.O., Moench, E., 2014. Data insight: which growth rate? It's a weighty subject. Federal Reserve Bank of New York, Liberty Street Economics .

Dahlhaus, T., Guenette, J.D., Vasishtha, G., 2017. Nowcasting BRIC+M in real time. International Journal of Forecasting 33, 915–935.

Del Negro, M., Eusepi, S., 2011. Fitting observed inflation expectations. Journal of Economic Dynamics and Control 35, 2105–2131.

Diebold, F.X., Mariano, R.S., 1995. Comparing Predictive Accuracy. Journal of Business & Economic Statistics 13, 253–263.

Durbin, J., Koopman, S.J., 2012. Time Series Analysis by State Space Methods. Number 38 in Oxford Statistical Science. 2nd ed., Oxford University Press.

Faust, J., Wright, J.H., 2009. Comparing Greenbook and Reduced Form Forecasts Using a Large Realtime Dataset. Journal of Business & Economic Statistics 27, 468–479.

Faust, J., Wright, J.H., 2013. Forecasting inflation, in: Handbook of Economic Forecasting. Elsevier, pp. 2–56.

Giacomini, R., White, H., 2006. Tests of Conditional Predictive Ability. Econometrica 74, 1545–1578.

Greenlees, J.S., Mason, C.C., 1996. Overview of the 1998 Revision of the Consumer Price Index. Monthly Labor Review December 1996. U.S. Bureau of Labor Statistics.

Harrison, J., West, M., 1997. Bayesian forecasting and dynamic models. Springer, New York.

Harrison, P.J., Stevens, C.F., 1975. Bayes forecasting in action: case studies. Department of Statistics Warwick Research Report 14. University of Warwick.

Jain, M., 2018. Sluggish Forecasts. Bank of Canada Staff Working Paper .

Jorda, O., 2005. Estimation and Inference of Impulse Responses by Local Projections. American Economic Review 95, 161–182.

Jorda, O., 2023. Local Projections for Applied Economics. Federal Reserve Bank of San Francisco Working Paper 2023-16.

Knotek II, E.S., Zaman, S., 2017. Nowcasting U.S. Headline and Core Inflation. Journal of Money, Credit and Banking 49, 931–968.

Lucas, R.E., 1976. Econometric policy evaluation: A critique. Carnegie-Rochester Conference Series on Public Policy 1, 19–46.

Mackowiak, B., Wiederholt, M., 2009. Optimal Sticky Prices under Rational Inattention. American Economic Review 99, 769–803.

Mankiw, N.G., Reis, R., 2002. Sticky Information versus Sticky Prices: A Proposal to Replace the New Keynesian Phillips Curve. The Quarterly Journal of Economics , 1295–1328.

Marcellino, M., Stock, J.H., Watson, M.W., 2006. A comparison of direct and iterated multistep AR methods for forecasting macroeconomic time series. Journal of Econometrics 135, 499–526.

Mariano, R.S., Murasawa, Y., 2003. A new coincident index of business cycles based on monthly and quarterly series. Journal of Applied Econometrics 18, 427–443.

McCracken, M.W., McGillicuddy, J.T., 2018. An empirical investigation of direct and iterated multistep conditional forecasts. Journal of Applied Econometrics 34, 181–204.

Mertens, E., Nason, J.M., 2018. Inflation and professional forecast dynamics: an evaluation of stickiness, persistence, and volatility. BIS Working Papers 713. Bank for International Settlements.

Monti, F., 2010. Combining Judgment and Models. Journal of Money, Credit and Banking 42, 1641–1662.

Nason, J.M., Smith, G.W., 2013. Reverse Kalman filtering U.S. inflation with sticky professional forecasts. Technical Report 13-34. Federal Reserve Bank of Philadelphia.

Patton, A.J., Timmermann, A., 2010. Why do forecasters disagree? Lessons from the term structure of cross-sectional dispersion. Journal of Monetary Economics 57, 803–820.

Patton, A.J., Timmermann, A., 2011. Predictability of Output Growth and Inflation: A Multi-Horizon Survey Approach. Journal of Business & Economic Statistics 29, 397–410.

Prado, R., West, M., 2010. Time Series: Modeling, Computation, and Inference. Chapman & Hall, London.

Rossi, B., Sekhposyan, T., 2015. Macroeconomic Uncertainty Indices Based on Nowcast and Forecast Error Distributions. American Economic Review 105, 650–655.

Schmitt-Grohe, S., Uribe, M., 2022. What Do Long Data Tell Us About the Inflation Hike Post COVID-19 Pandemic? NBER Working Papers .

Sims, C.A., 2003. Implications of rational inattention. Journal of Monetary Economics 50, 665–690.

Stock, J.H., Watson, M.W., 2007. Why Has U.S. Inflation Become Harder to Forecast? Journal of Money, Credit and Banking 39, 3–33.

Stock, J.H., Watson, M.W., 2010. Modeling Inflation After the Crisis. NBER Working Papers 16488. National Bureau of Economic Research, Inc.

Woodford, M., 2003. Imperfect Common Knowledge and the Effects of Monetary Policy, in: Knowledge, Information and Expectations in Modern Macroeconomics: Macroeconomics: In Honor of Edmund S. Phelps. Princeton: Princeton University Press. edited by Philippe Aghion, Roman Frydman, Joseph Stiglitz, and Michael Woodford, pp. 25–58.

A Derivations for Forecast Dominance

Kalman recursion applied to this model implies $\mathcal{F}_{i,q}\pi^{av}_{q+1+\mathfrak{h}} = \rho_{\mathfrak{h}}\mathcal{F}_{i,q}\pi^{av}_{q+\mathfrak{h}}$ and $\mathcal{F}_{q}\pi^{av}_{q+1+\mathfrak{h}} = \rho_{\mathfrak{h}}\mathcal{F}_{q}\pi^{av}_{q+\mathfrak{h}}$. Therefore, using (9) and (10), the Individual Forecast error $\xi_{i,q,\mathfrak{h}} \equiv \mathcal{F}_{i,q}\pi^{av}_{q+\mathfrak{h}} - \pi^{av}_{q+\mathfrak{h}}$ satisfies:

$$\begin{aligned}
\xi_{i,q,\mathfrak{h}} = \; & \mathcal{F}_{i,q}\pi^{av}_{q+\mathfrak{h}} - \pi^{av}_{q+\mathfrak{h}} = (1-\gamma_{\mathfrak{h}})\,\mathcal{F}_{i,q-1}\pi^{av}_{q+\mathfrak{h}} + \gamma_{\mathfrak{h}}E^{*}_{i,q}\pi^{av}_{q+\mathfrak{h}} - \pi^{av}_{q+\mathfrak{h}} \\
= \; & (1-\gamma_{\mathfrak{h}})\,\rho_{\mathfrak{h}}\mathcal{F}_{i,q-1}\pi^{av}_{q+\mathfrak{h}-1} + \gamma_{\mathfrak{h}}\left(\pi^{av}_{q+\mathfrak{h}} + \eta_{\mathfrak{h},q+\mathfrak{h}} + \delta_{i,\mathfrak{h},q+\mathfrak{h}}\right) - \pi^{av}_{q+\mathfrak{h}} \\
= \; & (1-\gamma_{\mathfrak{h}})\,\rho_{\mathfrak{h}}\mathcal{F}_{i,q-1}\pi^{av}_{q+\mathfrak{h}-1} - (1-\gamma_{\mathfrak{h}})\,\pi^{av}_{q+\mathfrak{h}} + \gamma_{\mathfrak{h}}\left(\eta_{\mathfrak{h},q+\mathfrak{h}} + \delta_{i,\mathfrak{h},q+\mathfrak{h}}\right) \\
= \; & (1-\gamma_{\mathfrak{h}})\left[\rho_{\mathfrak{h}}\mathcal{F}_{i,q-1}\pi^{av}_{q+\mathfrak{h}-1} - \pi^{av}_{q+\mathfrak{h}}\right] + \gamma_{\mathfrak{h}}\left(\eta_{\mathfrak{h},q+\mathfrak{h}} + \delta_{i,\mathfrak{h},q+\mathfrak{h}}\right) \\
= \; & (1-\gamma_{\mathfrak{h}})\left[\rho_{\mathfrak{h}}\mathcal{F}_{i,q-1}\pi^{av}_{q+\mathfrak{h}-1} - \rho_{\mathfrak{h}}\pi^{av}_{q+\mathfrak{h}-1} - \varepsilon_{\mathfrak{h},q+\mathfrak{h}}\right] + \gamma_{\mathfrak{h}}\left(\eta_{\mathfrak{h},q+\mathfrak{h}} + \delta_{i,\mathfrak{h},q+\mathfrak{h}}\right) \\
= \; & (1-\gamma_{\mathfrak{h}})\left(\rho_{\mathfrak{h}}\xi_{i,q-1,\mathfrak{h}} - \varepsilon_{\mathfrak{h},q+\mathfrak{h}}\right) + \gamma_{\mathfrak{h}}\left(\eta_{\mathfrak{h},q+\mathfrak{h}} + \delta_{i,\mathfrak{h},q+\mathfrak{h}}\right) \\
= \; & (1-\gamma_{\mathfrak{h}})\,\rho_{\mathfrak{h}}\xi_{i,q-1,\mathfrak{h}} - (1-\gamma_{\mathfrak{h}})\,\varepsilon_{\mathfrak{h},q+\mathfrak{h}} + \gamma_{\mathfrak{h}}\upsilon_{i,\mathfrak{h},q+\mathfrak{h}}
\end{aligned}$$

Since the Average Forecast error satisfies $\xi_{q,\mathfrak{h}} \equiv \int_0^1 \xi_{i,q,\mathfrak{h}}di$, and $\int_0^1 \upsilon_{i,\mathfrak{h},q+\mathfrak{h}}di = \eta_{\mathfrak{h},q+\mathfrak{h}}$, we obtain $\xi_{q,\mathfrak{h}} = (1-\gamma_{\mathfrak{h}})\,\rho_{\mathfrak{h}}\xi_{q-1,\mathfrak{h}} - (1-\gamma_{\mathfrak{h}})\,\varepsilon_{\mathfrak{h},q+\mathfrak{h}} + \gamma_{\mathfrak{h}}\eta_{\mathfrak{h},q+\mathfrak{h}}$. And lastly, since $E^{*}_{q}\pi^{av}_{q+\mathfrak{h}} = \pi^{av}_{q+\mathfrak{h}} + \eta_{\mathfrak{h},q+\mathfrak{h}}$, the Resetting Forecast error is $\xi^{*}_{q,\mathfrak{h}} \equiv E^{*}_{q}\pi^{av}_{q+\mathfrak{h}} - \pi^{av}_{q+\mathfrak{h}} = \eta_{\mathfrak{h},q+\mathfrak{h}}$.

As for Proposition 2, the proof is shown below.

Proposition 2 *Consider the modelling assumptions and results presented in Sections 5.1 and 5.2. In this case, the Resetting Forecast $E^{*}_{q}\pi^{av}_{q+\mathfrak{h}}$ has better forecasting performance than the Average Forecast $F_{q}\pi^{av}_{q+\mathfrak{h}}$ if and only if disagreement $\frac{\vartheta_{i,\mathfrak{h}}}{\vartheta_{\mathfrak{h}}}$ satisfies the following condition:*

$$\frac{2}{\left[1+\left(\bar{\sigma}^2/\vartheta_{\mathfrak{h}}\right)^{-1}\right]} < \frac{\vartheta_{i,\mathfrak{h}}}{\vartheta_{\mathfrak{h}}} < \frac{\bar{\sigma}^2}{\vartheta_{\mathfrak{h}}}$$

Proof. From Kalman recursion, we have:

$$\gamma_{\mathfrak{h}} = \frac{\kappa_{\mathfrak{h}}\bar{\sigma}^2}{\kappa_{\mathfrak{h}}\bar{\sigma}^2+\sigma^2_{\upsilon,\mathfrak{h}}} \quad ; \; \kappa_{\mathfrak{h}} = \frac{\left(1-\rho^2_{\mathfrak{h}}\right)}{2}\left[\left(1-\frac{\sigma^2_{\upsilon,\mathfrak{h}}}{\bar{\sigma}^2}\right) + \sqrt{\left(1-\frac{\sigma^2_{\upsilon,\mathfrak{h}}}{\bar{\sigma}^2}\right)^2 + \frac{4}{\left(1-\rho^2_{\mathfrak{h}}\right)}\frac{\sigma^2_{\upsilon,\mathfrak{h}}}{\bar{\sigma}^2}}\right]$$

Therefore, we obtain:

$$\kappa_{\mathfrak{h}} = \frac{\gamma_{\mathfrak{h}}}{\left(1-\gamma_{\mathfrak{h}}\right)}\frac{\sigma^2_{\upsilon,\mathfrak{h}}}{\bar{\sigma}^2} = \frac{\left(1-\rho^2_{\mathfrak{h}}\right)}{2}\left[\left(1-\frac{\sigma^2_{\upsilon,\mathfrak{h}}}{\bar{\sigma}^2}\right) + \sqrt{\left(1-\frac{\sigma^2_{\upsilon,\mathfrak{h}}}{\bar{\sigma}^2}\right)^2 + \frac{4}{\left(1-\rho^2_{\mathfrak{h}}\right)}\frac{\sigma^2_{\upsilon,\mathfrak{h}}}{\bar{\sigma}^2}}\right]$$

We then simplify the second equality into:

$$\therefore \bar{\sigma}^2 = \gamma_\mathfrak{h} \left[\frac{\gamma_\mathfrak{h}}{\left(1-\rho_\mathfrak{h}^2\right)\left(1-\gamma_\mathfrak{h}\right)} + 1 \right] \sigma_{\upsilon,\mathfrak{h}}^2 \tag{A.1}$$

From (11), we have:

$$\vartheta_{i,\mathfrak{h}} = \frac{\left(1-\gamma_\mathfrak{h}\right)^2\sigma_\mathfrak{h}^2+\left(\gamma_\mathfrak{h}\right)^2\sigma_{\upsilon,\mathfrak{h}}^2}{1-\left(1-\gamma_\mathfrak{h}\right)^2\rho_\mathfrak{h}^2} \quad ; \; \vartheta_\mathfrak{h} = \frac{\left(1-\gamma_\mathfrak{h}\right)^2\sigma_\mathfrak{h}^2+\left(\gamma_\mathfrak{h}\right)^2\sigma_{\eta,\mathfrak{h}}^2}{1-\left(1-\gamma_\mathfrak{h}\right)^2\rho_\mathfrak{h}^2} \quad ; \; \vartheta_\mathfrak{h}^* = \sigma_{\eta,\mathfrak{h}}^2 \tag{A.2}$$

Using $\vartheta_{i,\mathfrak{h}}$ in (A.2), $\bar{\sigma}^2$ in (A.1), and recalling that $\sigma_\mathfrak{h}^2 = \left(1-\rho_\mathfrak{h}^2\right)\bar{\sigma}^2$, we obtain:

$$\therefore \sigma_{\upsilon,\mathfrak{h}}^2 = \frac{1}{\gamma_\mathfrak{h}}\vartheta_{i,\mathfrak{h}} \tag{A.3}$$

And so, plugging the previous result for $\sigma_{\upsilon,\mathfrak{h}}^2$ back into (A.1), we obtain:

$$\rho_\mathfrak{h}^2 = 1 - \frac{\gamma_\mathfrak{h}}{\left(1-\gamma_\mathfrak{h}\right)\left(\frac{\bar{\sigma}^2}{\vartheta_{i,\mathfrak{h}}}-1\right)} \tag{A.4}$$

Using $\vartheta_\mathfrak{h}$ in (A.2), $\rho_\mathfrak{h}^2$ in (A.4), and recalling that $\sigma_\mathfrak{h}^2 = \left(1-\rho_\mathfrak{h}^2\right)\bar{\sigma}^2$, we obtain:

$$\sigma_{\eta,\mathfrak{h}}^2 = \frac{1}{\left(\frac{\bar{\sigma}^2}{\vartheta_{i,\mathfrak{h}}}-1\right)}\left[\left(\frac{\left(2-\gamma_\mathfrak{h}\right)}{\gamma_\mathfrak{h}}\frac{\bar{\sigma}^2}{\vartheta_{i,\mathfrak{h}}} - \frac{1}{\gamma_\mathfrak{h}}\right)\vartheta_\mathfrak{h} - \frac{\left(1-\gamma_\mathfrak{h}\right)}{\gamma_\mathfrak{h}}\bar{\sigma}^2\right] \tag{A.5}$$

If Resetting Forecasts dominate Average Forecasts, then $\vartheta_\mathfrak{h}^* < \vartheta_\mathfrak{h}$. Since $\vartheta_\mathfrak{h}^* = \sigma_{\eta,\mathfrak{h}}^2$, we obtain:

$$\frac{1}{\left(\frac{\bar{\sigma}^2}{\vartheta_{i,\mathfrak{h}}}-1\right)}\left[\left(\frac{\left(2-\gamma_\mathfrak{h}\right)}{\gamma_\mathfrak{h}}\frac{\bar{\sigma}^2}{\vartheta_{i,\mathfrak{h}}} - \frac{1}{\gamma_\mathfrak{h}}\right)\vartheta_\mathfrak{h} - \frac{\left(1-\gamma_\mathfrak{h}\right)}{\gamma_\mathfrak{h}}\bar{\sigma}^2\right] < \vartheta_\mathfrak{h} \tag{A.6}$$

Since $\rho_\mathfrak{h}^2 < 1$, equation (A.4) implies that $\left(\frac{\bar{\sigma}^2}{\vartheta_{i,\mathfrak{h}}}-1\right) > 0$. And so, (A.6) is equivalent to $\frac{2\bar{\sigma}^2}{\left(\bar{\sigma}^2+\vartheta_\mathfrak{h}\right)} < \frac{\vartheta_{i,\mathfrak{h}}}{\vartheta_\mathfrak{h}}$. Lastly, dividing by $\vartheta_\mathfrak{h}$, the inequality $\left(\frac{\bar{\sigma}^2}{\vartheta_{i,\mathfrak{h}}}-1\right) > 0$ can be rewritten as $\frac{\vartheta_{i,\mathfrak{h}}}{\vartheta_\mathfrak{h}} < \frac{\bar{\sigma}^2}{\vartheta_\mathfrak{h}}$. Therefore, we obtain the following condition:

$$\frac{2}{\left[1+\left(\bar{\sigma}^2/\vartheta_\mathfrak{h}\right)^{-1}\right]} < \frac{\vartheta_{i,\mathfrak{h}}}{\vartheta_\mathfrak{h}} < \frac{\bar{\sigma}^2}{\vartheta_\mathfrak{h}}$$

■

Online Appendix

B Average-Price Rate

We aim to derive a log-linearized map between $\Pi_t^{av}$and Π_t. For that, lower case variables correspond to log-linearized versions of the original upper case variables, e.g. $\varkappa_t \equiv \log(\mathcal{X}_t)$. Therefore, we have $\pi_t = p_t - p_{t-1}$ and $\pi_t^{av} = p_t^{av} - p_{t-3}^{av}$. As for P_t^{av}, we must use a first-order log-approximation centered at P_t:

$$\begin{aligned} P_t\left[p_t^{av} - \log(P_t)\right] \approx & \quad \tfrac{1}{3}P_t\left(\left[p_{t+1} - \log(P_t)\right] + \left[p_t - \log(P_t)\right] + \left[p_{t-1} - \log(P_t)\right]\right) \\ \therefore p_t^{av} \approx & \quad \tfrac{1}{3}\left(p_{t+1} + p_t + p_{t-1}\right) \end{aligned}$$

which implies $\pi_t^{av} \approx \frac{1}{3}\left(p_{t+1} + p_t + p_{t-1}\right) - \frac{1}{3}\left(p_{t-2} + p_{t-3} + p_{t-4}\right)$. Since $\pi_t = p_t - p_{t-1}$, we obtain $\pi_t^{av} \approx \frac{1}{3}\left[\pi_{t+1} + 2\pi_t + 3\pi_{t-1} + 2\pi_{t-2} + \pi_{t-3}\right]$.

C Forecast Dynamics for Longer Horizons

Proposition 1 *If the degree of forecast rigidity for any horizon $h \geq H+3$ is constant, with $H \geq 0$, and there is no extra information disturbances for those longer horizons, i.e. $\alpha_h = \bar{\alpha}$ and $s_{h,t}^{av} = 0$ for $h \in \{H+3, H+6, ...\}$, then $F_t\pi_{t+h}^{av}$ evolves according to an autoregressive system that does not depend on lagged forecasts for longer horizons:*

$$\begin{aligned} \mathcal{F}_t\pi_{t+h}^{av} &= \mathcal{F}_t\pi_{t+h}^{amr.} + \mathcal{F}_t\pi_{t+h}^{asr} + \mathcal{F}_t\pi_{t+h}^{alr} \\ \text{where} & \\ \mathcal{F}_t\pi_{t+h}^{amr.} &= (1-\bar{\alpha})\,E_{t-2}\pi_{t+h}^{amr} + \bar{\alpha}\left(\rho_{mr}\right)^3\mathcal{F}_{t-3}\pi_{t-3+h}^{amr} \\ \mathcal{F}_t\pi_{t+h}^{asr.} &= (1-\bar{\alpha})\,E_{t-2}\pi_{t+h}^{asr} + \bar{\alpha}\left(\rho_{sr}\right)^3\mathcal{F}_{t-3}\pi_{t-3+h}^{asr} \\ \mathcal{F}_t\pi_{t+h}^{alr} &= (1-\bar{\alpha})\,E_{t-2}\pi_{t+h}^{alr} + \bar{\alpha}\mathcal{F}_{t-3}\pi_{t-3+h}^{alr} \\ \pi_{t+h}^{amr} &\equiv \tfrac{1}{3}\left[\pi_{t+h+1}^{mr} + 2\pi_{t+h}^{mr} + 3\pi_{t+h-1}^{mr} + 2\pi_{t+h-2}^{mr} + \pi_{t+h-3}^{mr}\right] \\ \pi_{t+h}^{asr} &\equiv \tfrac{1}{3}\left[\pi_{t+h+1}^{sr} + 2\pi_{t+h}^{sr} + 3\pi_{t+h-1}^{sr} + 2\pi_{t+h-2}^{sr} + \pi_{t+h-3}^{sr}\right] \\ \pi_{t+h}^{alr} &\equiv \tfrac{1}{3}\left[\pi_{t+h+1}^{lr} + 2\pi_{t+h}^{lr} + 3\pi_{t+h-1}^{lr} + 2\pi_{t+h-2}^{lr} + \pi_{t+h-3}^{lr}\right] \end{aligned}$$

Proof If $\alpha_h = \bar{\alpha}$ and $\mathfrak{s}_{h,t} = 0$ for $h \in \{H+3, H+6, ...\}$ and $H \geq 0$, with a forecast rule $E_t^*\pi_{t+h}^{av} = E_{t-2}\pi_{t+h}^{av} + \mathfrak{s}_{h,t}$, then the law of motion of the aggregate forecast is described as $\mathcal{F}_t\pi_{t+h}^{av} =$

$(1-\bar{\alpha})\,E_{t-2}\pi^{av}_{t+h} + \bar{\alpha}\mathcal{F}_{t-3}\pi^{av}_{t+h}$. Using the lag operator (L), we can expand the equation as follows:

$$\begin{aligned}
\mathcal{F}_t\pi^{av}_{t+h} &= (1-\bar{\alpha})\,E_{t-2}\pi^{av}_{t+h} + \bar{\alpha}\mathcal{F}_{t-3}\pi^{av}_{t+h} = (1-\bar{\alpha})\,E_{t-2}\pi^{av}_{t+h} + \bar{\alpha}L^3\mathcal{F}_t\pi^{av}_{t+h+3} \\
&= (1-\bar{\alpha})\,E_{t-2}\pi^{av}_{t+h} + (1-\bar{\alpha})\,\bar{\alpha}E_{t-5}\pi^{av}_{t+h} + \bar{\alpha}^2L^6\mathcal{F}_t\pi^{av}_{t+h+6} \\
&= (1-\bar{\alpha})\,E_{t-2}\pi^{av}_{t+h} + (1-\bar{\alpha})\,\bar{\alpha}E_{t-5}\pi^{av}_{t+h} + (1-\bar{\alpha})\,\bar{\alpha}^2E_{t-8}\pi^{av}_{t+h} + \bar{\alpha}^3L^9\mathcal{F}_t\pi^{av}_{t+h+9} \\
&= ...
\end{aligned}$$

Therefore, we obtain:

$$\mathcal{F}_t\pi^{av}_{t+h} = (1-\bar{\alpha})\left(E_{t-2}\pi^{av}_{t+h}\right) + (1-\bar{\alpha})\sum_{v=1}^{\infty}(\bar{\alpha})^v\,E_{(t-2-3v)}\pi^{av}_{t+h} = (1-\bar{\alpha})\sum_{v=0}^{\infty}(\bar{\alpha})^v\,E_{(t-2-3v)}\pi^{av}_{t+h}$$

where:

$$\begin{aligned}
E_{(t-2-3v)}\pi^{av}_{t+h} &= E_{(t-2-3v)}\tfrac{1}{3}\left[\pi^{sa}_{t+h+1} + 2\pi^{sa}_{t+h} + 3\pi^{sa}_{t+h-1} + 2\pi^{sa}_{t+h-2} + \pi^{sa}_{t+h-3}\right] \\
&= E_{(t-2-3v)}\tfrac{1}{3}\left[\pi^{mr}_{t+h+1} + 2\pi^{mr}_{t+h} + 3\pi^{mr}_{t+h-1} + 2\pi^{mr}_{t+h-2} + \pi^{mr}_{t+h-3}\right] \\
&\quad + E_{(t-2-3v)}\tfrac{1}{3}\left[\pi^{sr}_{t+h+1} + 2\pi^{sr}_{t+h} + 3\pi^{sr}_{t+h-1} + 2\pi^{sr}_{t+h-2} + \pi^{sr}_{t+h-3}\right] \\
&\quad + E_{(t-2-3v)}\tfrac{1}{3}\left[\pi^{lr}_{t+h+1} + 2\pi^{lr}_{t+h} + 3\pi^{lr}_{t+h-1} + 2\pi^{lr}_{t+h-2} + \pi^{lr}_{t+h-3}\right]
\end{aligned}$$

Up to this point, the result is general and does not require $H \geq 0$. However, in order to proceed we must know whether period $(t-2-3v)$ belongs to the past or future of each inflation timing in the last result, from $(t+h-3)$ to $(t+h+1)$. Now, using the assumptions $h \geq H+3$ and $H \geq 0$, we show below that $(t-2-3v)$ is actually smaller than the smallest timing $(t+h-3)$. Indeed, notice that $(t+h-3) \geq (t+H+3-3) = (t+H) \geq t \geq t-2-3v$. With that result, it makes it easier to compute expectations when considering the DGP dynamic equations:

$$\begin{aligned}
\pi^{sa}_t = \pi^{mr}_t + \pi^{sr}_t + \pi^{lr}_t \quad &; \; \pi^{mr}_t = \rho_{mr}\pi^{mr}_{t-1} + \varepsilon^{mr}_t \\
\pi^{lr}_t = \pi^{lr}_{t-1} + \varepsilon^{lr}_t \quad &; \; \pi^{sr}_t = \rho_{sr}\pi^{sr}_{t-1} + \varepsilon^{sr}_t
\end{aligned}$$

Their dynamics imply that:

$$\begin{aligned}
E_{(t-2-3v)}\pi^{av}_{t+h} &= (\rho_{mr})^{h-1+3v}\,\tfrac{1}{3}\left[(\rho_{mr})^4 + 2\,(\rho_{mr})^3 + 3\,(\rho_{mr})^2 + 2\,(\rho_{mr}) + 1\right]\pi^{mr}_{t-2-3v} \\
&\quad + (\rho_{sr})^{h-1+3v}\,\tfrac{1}{3}\left[(\rho_{sr})^4 + 2\,(\rho_{sr})^3 + 3\,(\rho_{sr})^2 + 2\,(\rho_{sr}) + 1\right]\pi^{mr}_{t-2-3v} \\
&\quad + \tfrac{1}{3}\left[1+2+3+2+1\right]\pi^{lr}_{t-2-3v}
\end{aligned}$$

Since $\mathcal{F}_t\pi^{av}_{t+h} = (1-\bar{\alpha})\sum_{v=0}^{\infty}(\bar{\alpha})^v\,E_{(t-2-3v)}\pi^{av}_{t+h}$, we decompose $\mathcal{F}_t\pi^{av}_{t+h}$ into three terms:

$$\mathcal{F}_t\pi^{av}_{t+h} = \mathcal{F}_t\pi^{amr.}_{t+h} + \mathcal{F}_t\pi^{asr}_{t+h} + \mathcal{F}_t\pi^{alr}_{t+h}$$

where

$$\begin{aligned}
\mathcal{F}_t\pi^{amr.}_{t+h} &= \tfrac{(1-\bar{\alpha})\Phi_{h,h}}{3}\sum_{v=0}^{\infty}\left(\bar{\alpha}\left(\rho_{mr}\right)^3\right)^v\pi^{mr}_{t-2-3v}\\
\mathcal{F}_t\pi^{asr}_{t+h} &= \tfrac{(1-\bar{\alpha})\Phi_{l,h}}{3}\sum_{v=0}^{\infty}\left(\bar{\alpha}\left(\rho_{sr}\right)^3\right)^v\pi^{sr}_{t-2-3v}\\
\mathcal{F}_t\pi^{alr}_{t+h} &= \tfrac{(1-\bar{\alpha})\Phi_{lr}}{3}\sum_{v=0}^{\infty}\left(\bar{\alpha}\right)^v\pi^{lr}_{t-2-3v}
\end{aligned}$$

and $\Phi_{h,h}$, $\Phi_{l,h}$ and Φ_{lr} are auxiliary parameters:

$$\begin{aligned}
\Phi_{h,h} &= \left(\rho_{mr}\right)^{h-1}\left[\left(\rho_{mr}\right)^4+2\left(\rho_{mr}\right)^3+3\left(\rho_{mr}\right)^2+2\left(\rho_{mr}\right)+1\right]=\left(\rho_{mr}\right)^{h-1}\left[\left(\rho_{mr}\right)^2+\left(\rho_{mr}\right)+1\right]^2\\
\Phi_{l,h} &= \left(\rho_{sr}\right)^{h-1}\left[\left(\rho_{sr}\right)^4+2\left(\rho_{sr}\right)^3+3\left(\rho_{sr}\right)^2+2\left(\rho_{sr}\right)+1\right]=\left(\rho_{sr}\right)^{h-1}\left[\left(\rho_{sr}\right)^2+\left(\rho_{sr}\right)+1\right]^2\\
\Phi_{lr} &= [1+2+3+2+1]=9
\end{aligned}$$

We can work on those components as follows:

$$\begin{aligned}
\mathcal{F}_t\pi^{amr.}_{t+h} &= \tfrac{(1-\bar{\alpha})\Phi_{h,h}}{3}\sum_{v=0}^{\infty}\left(\bar{\alpha}\left(\rho_{mr}\right)^3\right)^v\pi^{mr}_{t-2-3v}\\
&= \tfrac{(1-\bar{\alpha})\Phi_{h,h}}{3}\pi^{mr}_{t-2}+\tfrac{(1-\bar{\alpha})\Phi_{h,h}}{3}\sum_{v=1}^{\infty}\left(\bar{\alpha}\left(\rho_{mr}\right)^3\right)^v\pi^{mr}_{t-2-3v}\\
&= \tfrac{(1-\bar{\alpha})\Phi_{h,h}}{3}\pi^{mr}_{t-2}+\overbrace{\bar{\alpha}\left(\rho_{mr}\right)^3\frac{\left(1-\bar{\alpha}\right)\Phi_{h,h}}{3}\sum_{V=0}^{\infty}\left(\bar{\alpha}\left(\rho_{mr}\right)^3\right)^V\pi^{mr}_{(t-3)-2-3V}}^{V=v-1}\\
&= \tfrac{(1-\bar{\alpha})\Phi_{h,h}}{3}\pi^{mr}_{t-2}+\bar{\alpha}\left(\rho_{mr}\right)^3\mathcal{F}_{(t-3)}\pi^{amr}_{(t-3)+h}
\end{aligned}$$

Analogously, we have:

$$\begin{aligned}
\mathcal{F}_t\pi^{asr.}_{t+h} &= \tfrac{(1-\bar{\alpha})\Phi_{l,h}}{3}\pi^{sr}_{t-2}+\bar{\alpha}\left(\rho_{sr}\right)^3\mathcal{F}_{(t-3)}\pi^{asr}_{(t-3)+h}\\
\mathcal{F}_t\pi^{alr}_{t+h} &= \tfrac{(1-\bar{\alpha})\Phi_{lr}}{3}\pi^{lr}_{t-2}+\bar{\alpha}\left(\rho_{sr}\right)^3\mathcal{F}_{(t-3)}\pi^{lr}_{(t-3)+h}
\end{aligned}$$

Using the definitions of $\Phi_{h,h}$, $\Phi_{l,h}$ and Φ_{lr}, note now that

$$\begin{aligned}
\tfrac{\Phi_{h,h}\pi^{mr}_{t-2}}{3} &= \tfrac{1}{3}\left(\rho_{mr}\right)^{h-1}\left[\left(\rho_{mr}\right)^4+2\left(\rho_{mr}\right)^3+3\left(\rho_{mr}\right)^2+2\left(\rho_{mr}\right)+1\right]\pi^{mr}_{t-2}\\
&= \tfrac{1}{3}\left[\left(\rho_{mr}\right)^{h+3}\pi^{mr}_{t-2}+2\left(\rho_{mr}\right)^{h+2}\pi^{mr}_{t-2}+3\left(\rho_{mr}\right)^{h+1}\pi^{mr}_{t-2}+2\left(\rho_{mr}\right)^{h}\pi^{mr}_{t-2}+\left(\rho_{mr}\right)^{h-1}\pi^{mr}_{t-2}\right]\\
&= \tfrac{1}{3}E_{t-2}\left[\pi^{mr}_{t+h+1}+2\pi^{mr}_{t+h}+3\pi^{mr}_{t+h-1}+2\pi^{mr}_{t+h-2}+\pi^{mr}_{t+h-3}\right]=E_{t-2}\pi^{amr}_{t+h}
\end{aligned}$$

Analogously, we have $\frac{\Phi_{l,h}}{3}\pi^{sr}_{t-2}=E_{t-2}\pi^{asr}_{t+h}$ and $\frac{\Phi_{lr}}{3}\pi^{lr}_{t-2}=E_{t-2}\pi^{alr}_{t+h}$. Therefore, under the

assumed conditions, the dynamics of $\mathcal{F}_t\pi^{av}_{t+h}$ can be described as follows:

$$\begin{aligned}
\mathcal{F}_t\pi^{av}_{t+h} &= \mathcal{F}_t\pi^{amr.}_{t+h} + \mathcal{F}_t\pi^{asr}_{t+h} + \mathcal{F}_t\pi^{alr}_{t+h} \\
\mathcal{F}_t\pi^{amr.}_{t+h} &= (1-\bar{\alpha})\, E_{t-2}\pi^{amr}_{t+h} + \bar{\alpha}\,(\rho_{mr})^3\, \mathcal{F}_{t-3}\pi^{amr}_{t-3+h} \\
\mathcal{F}_t\pi^{asr.}_{t+h} &= (1-\bar{\alpha})\, E_{t-2}\pi^{asr}_{t+h} + \bar{\alpha}\,(\rho_{sr})^3\, \mathcal{F}_{t-3}\pi^{asr}_{t-3+h} \\
\mathcal{F}_t\pi^{alr}_{t+h} &= (1-\bar{\alpha})\, E_{t-2}\pi^{alr}_{t+h} + \bar{\alpha}\mathcal{F}_{t-3}\pi^{alr}_{t-3+h}
\end{aligned}$$

$$\begin{aligned}
\pi^{amr}_{t+h} &\equiv \tfrac{1}{3}\left[\pi^{mr}_{t+h+1} + 2\pi^{mr}_{t+h} + 3\pi^{mr}_{t+h-1} + 2\pi^{mr}_{t+h-2} + \pi^{mr}_{t+h-3}\right] \\
\pi^{asr}_{t+h} &\equiv \tfrac{1}{3}\left[\pi^{sr}_{t+h+1} + 2\pi^{sr}_{t+h} + 3\pi^{sr}_{t+h-1} + 2\pi^{sr}_{t+h-2} + \pi^{sr}_{t+h-3}\right] \\
\pi^{alr}_{t+h} &\equiv \tfrac{1}{3}\left[\pi^{lr}_{t+h+1} + 2\pi^{lr}_{t+h} + 3\pi^{lr}_{t+h-1} + 2\pi^{lr}_{t+h-2} + \pi^{lr}_{t+h-3}\right]
\end{aligned}$$

D Estimated Forecast System

As for the zero-meaned monthly complementary forecasting components $\mathfrak{s}_{h,t}$, which we model as white-noise components, we need an extra assumption for very distant horizons. Recall that $h = 12$ is the furthest horizon for which we have observed SPF quarterly forecasts, i.e. for $\mathcal{F}_t\pi^{av}_{t+12}$. At this horizon, the aggregate component $\mathfrak{s}^{av}_{12,t}$ depends on complementary forecasting components from $\mathfrak{s}_{9,t}$ to $\mathfrak{s}_{13,t}$. Therefore, we impose $\mathfrak{s}_{h,t} = 0$ for $\forall h \geq 14$ in order for $\mathfrak{s}_{13,t}$ to be the furthest complementary forecasting component whose distribution will be retrieved by the Kalman filter during estimation. In the same line, we impose a similar restriction for distant past horizons. Since we observe $\mathcal{F}_t\pi^{av}_{t-3}$, the aggregate component $\mathfrak{s}^{av}_{-3,t}$ depends on complementary forecasting components from $\mathfrak{s}_{-2,t}$ to $\mathfrak{s}_{-6,t}$. At the pivot month t, however, the previous quarter regards months $(t-2)$ to $(t-4)$. Therefore, we assume $\mathfrak{s}_{h,t} = 0$ for $\forall h \leq -5$. That is, we only allow for non-zero components $\mathfrak{s}_{h,t}$ at quarterly horizons surveyed by SPF. In a nutshell, we impose $\mathfrak{s}_{h,t} = 0$ for $\forall h \geq 14$ and $\forall h \leq -5$.

For identification purposes, we also impose that monthly forecasting components related to the same SPF quarterly horizon are equal. That is, for any horizon $h \in \{-3, 0, 3, 6, 9, 12\}$, we set $\mathfrak{s}_{h+1,t} = \mathfrak{s}_{h,t}$ and $\mathfrak{s}_{h-1,t} = \mathfrak{s}_{h,t}$. Lastly, for inference pragmatism, we need assumptions to simplify estimation in this mixed-frequency estimation environment, as SPF information is much more sparse than monthly information. Even though $\mathfrak{s}_{h,t}$ varies in time and is different for each horizon, we assume all of them have the same horizon-invariant variance $\sigma^2_{\mathfrak{s}}$, i.e. $\mathfrak{s}_{h,t} \sim N\left(0, \sigma^2_{\mathfrak{s}}\right)$. We assume all rigidity parameters for distant horizons are the same as that of horizon $h = 12$. That is, we assume $\alpha_h = \alpha_{12}$ for $\forall h \geq 12$. Even imposing the restriction $\mathfrak{s}_{h,t} = 0$ for $\forall h \geq 14$,

note that $\mathfrak{s}_{13,t}$ and $\mathfrak{s}_{12,t}$ are still affecting $\mathfrak{s}^{av}_{15,t}$. Therefore, $\mathfrak{s}_{13,t}$ and $\mathfrak{s}_{12,t}$ hit the dynamics of the non-observed forecast $\mathcal{F}_t\pi^{av}_{t+15}$. Since this forecast depends on the 3-month lagged value of the also non-observed forecast $\mathcal{F}_t\pi^{av}_{t+18}$, we proceed as follows. We let $\mathcal{F}_t\pi^{av}_{t+15}$ process be described by (6), while the dynamics of $\mathcal{F}_t\pi^{av}_{t+18}$ is described by (7).

Below, we show how those inference assumptions affect the estimated forecast system. Quarterly aggregation quantities, for $h \in \{-3, 0, 3, 6, 9, 12\}$ are $\mathcal{F}_t\pi^{av}_{t+h}$, $E^*_t\pi^{av}_{t+h}$ and $\mathfrak{s}_{h,t}$. Monthly aggregation quantities, for $j \in \{-6, ..., -2, -1, 0, 1, 2, ..., 18\}$, are $E^*_t\pi^{sa}_{t+j}$ and $E_{t-2}\pi^{sa}_{t+j}$.

$h = -6$:

$$
\begin{aligned}
E^*_t\pi^{sa}_{t-6} &= \pi^{sa}_{t-6} \;\; ; \;\; E^*_t\pi^{sa}_{t-5} = \pi^{sa}_{t-5}
\end{aligned}
$$

$h = -3$:

$$
\begin{aligned}
\mathcal{F}_t\pi^{av}_{t-3} &= (1-\alpha_{-3})\, E^*_t\pi^{av}_{t-3} + \alpha_{-3}\mathcal{F}_{t-3}\pi^{av}_{t-3} \\
E^*_t\pi^{av}_{t-3} &= \tfrac{1}{3}\left[E^*_t\pi^{sa}_{t-2} + 2E^*_t\pi^{sa}_{t-3} + 3E^*_t\pi^{sa}_{t-4} + 2E^*_t\pi^{sa}_{t-5} + E^*_t\pi^{sa}_{t-6}\right] \\
E^*_t\pi^{sa}_{t-4} &= \pi^{sa}_{t-4} + \mathfrak{s}_{-3,t} \;\; ; \;\; E^*_t\pi^{sa}_{t-3} = \pi^{sa}_{t-3} + \mathfrak{s}_{-3,t} \;\; ; \;\; E^*_t\pi^{sa}_{t-2} = \pi^{sa}_{t-2} + \mathfrak{s}_{-3,t} \\
\mathfrak{s}_{-3,t} &\sim N\left(0, \sigma^2_{\mathfrak{s}}\right)
\end{aligned}
$$

$h = 0$:

$$
\begin{aligned}
\mathcal{F}_t\pi^{av}_{t} &= (1-\alpha_{0})\, E^*_t\pi^{av}_{t} + \alpha_{0}\mathcal{F}_{t-3}\pi^{av}_{t} \\
E^*_t\pi^{av}_{t} &= \tfrac{1}{3}\left[E^*_t\pi^{sa}_{t+1} + 2E^*_t\pi^{sa}_{t} + 3E^*_t\pi^{sa}_{t-1} + 2E^*_t\pi^{sa}_{t-2} + E^*_t\pi^{sa}_{t-3}\right] \\
E^*_t\pi^{sa}_{t+1} &= E_{t-2}\pi^{sa}_{t+1} + \mathfrak{s}_{0,t} \;\; ; \;\; E^*_t\pi^{sa}_{t} = E_{t-2}\pi^{sa}_{t} + \mathfrak{s}_{0,t} \;\; ; \;\; E^*_t\pi^{sa}_{t-1} = E_{t-2}\pi^{sa}_{t-1} + \mathfrak{s}_{0,t} \\
\mathfrak{s}_{0,t} &\sim N\left(0, \sigma^2_{\mathfrak{s}}\right)
\end{aligned}
$$

$\vdots$

$h = 12$:

$$
\begin{aligned}
\mathcal{F}_t\pi^{av}_{t+12} &= (1-\alpha_{12})\, E^*_t\pi^{av}_{t+12} + \alpha_{12}\mathcal{F}_{t-3}\pi^{av}_{t+12} \\
E^*_t\pi^{av}_{t+12} &= \tfrac{1}{3}\left[E^*_t\pi^{sa}_{t+13} + 2E^*_t\pi^{sa}_{t+12} + 3E^*_t\pi^{sa}_{t+11} + 2E^*_t\pi^{sa}_{t+10} + E^*_t\pi^{sa}_{t+9}\right] \\
E^*_t\pi^{sa}_{t+13} &= E_{t-2}\pi^{sa}_{t+13} + \mathfrak{s}_{12,t} \;\; ; \;\; E^*_t\pi^{sa}_{t+12} = E_{t-2}\pi^{sa}_{t+12} + \mathfrak{s}_{12,t} \\
E^*_t\pi^{sa}_{t+11} &= E_{t-2}\pi^{sa}_{t+11} + \mathfrak{s}_{12,t} \\
\mathfrak{s}_{12,t} &\sim N\left(0, \sigma^2_{\mathfrak{s}}\right)
\end{aligned}
$$

$h = 15$:

$$
\begin{aligned}
\mathcal{F}_t\pi^{av}_{t+15} &= (1-\alpha_{12})\, E^*_t\pi^{av}_{t+15} + \alpha_{12}\mathcal{F}_{t-3}\pi^{av}_{t+15} \\
E^*_t\pi^{av}_{t+15} &= \tfrac{1}{3}\left[E^*_t\pi^{sa}_{t+16} + 2E^*_t\pi^{sa}_{t+15} + 3E^*_t\pi^{sa}_{t+14} + 2E^*_t\pi^{sa}_{t+13} + E^*_t\pi^{sa}_{t+12}\right] \\
E^*_t\pi^{sa}_{t+16} &= E_{t-2}\pi^{sa}_{t+16} \;\; ; \;\; E^*_t\pi^{sa}_{t+15} = E_{t-2}\pi^{sa}_{t+15} \;\; ; \;\; E^*_t\pi^{sa}_{t+14} = E_{t-2}\pi^{sa}_{t+14}
\end{aligned}
$$

$h = 18$:

$$\begin{aligned}
\mathcal{F}_t \pi_{t+18}^{av} &= \mathcal{F}_t \pi_{t+18}^{amr.} + \mathcal{F}_t \pi_{t+18}^{asr} + \mathcal{F}_t \pi_{t+18}^{alr} \\
\mathcal{F}_t \pi_{t+18}^{amr.} &= (1-\alpha_{12}) E_{t-2} \pi_{t+18}^{amr} + \alpha_{12} (\rho_{mr})^3 \mathcal{F}_{t-3} \pi_{t-3+18}^{amr} \\
\mathcal{F}_t \pi_{t+18}^{asr.} &= (1-\alpha_{12}) E_{t-2} \pi_{t+18}^{asr} + \alpha_{12} (\rho_{sr})^3 \mathcal{F}_{t-3} \pi_{t-3+18}^{asr} \\
\mathcal{F}_t \pi_{t+18}^{alr} &= (1-\alpha_{12}) E_{t-2} \pi_{t+18}^{alr} + \alpha_{12} \mathcal{F}_{t-3} \pi_{t-3+18}^{alr} \\
E_{t-2} \pi_{t+18}^{amr} &= \tfrac{1}{3} E_{t-2} \left[\pi_{t+19}^{mr} + 2\pi_{t+18}^{mr} + 3\pi_{t+17}^{mr} + 2\pi_{t+16}^{mr} + \pi_{t+15}^{mr} \right] \\
E_{t-2} \pi_{t+18}^{asr} &= \tfrac{1}{3} E_{t-2} \left[\pi_{t+19}^{sr} + 2\pi_{t+18}^{sr} + 3\pi_{t+17}^{sr} + 2\pi_{t+16}^{sr} + \pi_{t+15}^{sr} \right] \\
E_{t-2} \pi_{t+18}^{alr} &= \tfrac{1}{3} E_{t-2} \left[\pi_{t+19}^{lr} + 2\pi_{t+18}^{lr} + 3\pi_{t+17}^{lr} + 2\pi_{t+16}^{lr} + \pi_{t+15}^{lr} \right]
\end{aligned}$$